Int. J. Multiphase Flow Vol. 19, No. 2, pp. 245–280, 1993
Printed in Great Britain.

0301-9322/93 $6.00 + 0.00

FLOW REGIMES IN TWO-PHASE GAS–LIQUID FLOW

P. L. SPEDDING[1] and D. R. SPENCE[2]

[1]Department of Chemical Engineering, The Queen's University of Belfast, Belfast BT9 5AG, N. Ireland

[2]Du Pont Ltd, Maydown Works, Campsie, Londonderry BT47 1TU, N. Ireland

(Received 25 April 1991; in revised form 29 November 1992)

Abstract—Experimental data were determined for co-current air–water horizontal flow in a 0.0935 m i.d. pipe. The flow patterns were identified by a combination of visual/video observations, the pressure fluctuation characteristics and a detailed examination of the pressure loss and holdup data. The results together with previous work at 0.0454 m i.d. were used to test existing flow regime maps. Several of the maps did not predict correctly the flow regimes for the two diameters. Theoretical and empirical models developed for the prediction of flow pattern transitions were also proved to be deficient in handling changes in physical properties and geometry. Thus, a need was shown to exist to develop a more satisfactory method of phase transition prediction.

Key Words: two-phase flow, gas–liquid co-current flow, flow patterns, flow pattern identification, flow pattern maps, flow pattern transitions

INTRODUCTION

A number of distinct flow patterns occur when gas and liquid pass co-currently through a pipe but the exact pattern that is formed depends on the basic mechanism acting within the conduit (Vohr 1960). Vohr emphasized that it was essential to ensure correct identification and definition of regimes and attempted to rationalize the situation. Spedding & Nguyen (1980) described the flow regimes expected in horizontal flow for a 0.0454 m i.d. pipe and showed that flow pattern formation depended to some degree on the initial height of liquid flowing in the pipe. However, the most commonly accepted definitions of flow patterns are those presented by Mandhane *et al.* (1974), which ignored some of the more elusive regimes. Lin & Hanratty (1987a) have recently pointed out that a number of flow regimes existed between those given by Mandhane *et al.* (1974) and have provided a plausible explanation as to why such regimes have failed to be observed by some workers. Lin & Hanratty (1987b) modified the pressure fluctuation technique of Dukler & Hubbard (1975), used to characterize flow regimes, and thus lent support to visual observation of the patterns and their transitions.

Many different types of flow regime maps have been developed for the prediction of flow patterns under various conditions of flow. Kosterin (1949) was possibly the first to suggest the use of regime maps and used a technique of presentation that later was extended by Hoogendoorn (1959). Spedding & Nguyen (1980) and Troniewski & Ulbrich (1984) have reviewed the various parameters which can be employed as mapping factors. By far the largest number of workers (ca. 17) have used the superficial phase velocities, in one form or another, as mapping parameters. Others have used either the mass flow rates (ca. 4) or mass velocity expression (ca. 9) for defining flow regime maps. A small number of workers (ca. 8) have employed dimensionless groups, mainly the Fr (Froude number), as the main mapping parameter. Thus, there exists no agreement as to the most useful mapping parameters to be employed in any flow regime map.

The most widely accepted regime map is that suggested by Mandhane *et al.* (1974) which uses the superficial phase velocities as mapping parameters. Taitel & Dukler (1976a) developed a mechanistic approach to derive the basic map from a fundamental level, while Weisman *et al.* (1979) and Barnea *et al.* (1980b, 1982, 1983; Barnea & Brauner 1985; Barnea & Taitel 1986; Barnea 1987) have extended the general approach to include the effects of geometric and operational variables. However, there appears to be some degree of disagreement amongst investigators about some of the transitions between flow regimes and the mechanisms which are involved. For example, Lin & Hanratty (1987a) showed that the Mandhane *et al.* (1974) map did not account for the effect

of diameter correctly. The same was true of the theoretical extension of the map suggested by Taitel & Dukler (1976a, b). Further, Lin & Hanratty (1987a) have shown that Fr was the most appropriate parameter for correlation of the onset of atomization and the transition to slug (S) flow at relatively high gas velocities.

Clearly there exists a number of problems with identifying and defining flow regimes and establishing their range of operation as well as with determining the most appropriate mapping parameter and form of regime map that will handle variations in phase parameters and system geometry. It is the object of this work to attempt to rectify this unsatisfactory situation.

EXPERIMENTAL

Pressure drop, holdup and flow pattern data were obtained for two-phase air and water co-current flow in a 0.0935 m i.d., 2.021 m long horizontal perspex pipe test section set 4.041 m from the exit of the gas–liquid mixer. The rig is shown schematically in figure 1.

Air flow rates of up to 575 kg h^{-1} and water flow rates of up to 9600 kg h^{-1} could be accommodated. The air and water were metered using either an orifice meter or a rotameter and then mixed in an annular mixing section, consisting of an outer piezometric ring which received the water into the annulus and conveyed it as a series of jets through holes into the air stream in the main test section. Thus, the mixer design set up intense air water contact in the mixing section that ensured the flow settled down to its final state within a length-to-diameter (l/d) ratio of 40. The air and water mixture emerging from the pipe was separated in a cyclone which was arranged to avoid pressure waves passing back up the pipe. The whole apparatus was held rigidly in supports so as to eliminate any movement. Figure 2 details the test section.

Holdup was measured by mechanically isolating the test section using two synchronously operating gate valves and subsequently measuring the volume of water held between them. This method has been recommended by Gay *et al.* (1978) and Hewitt (1982) as being the most accurate for the measurement of holdup. A correction of about 100 g was applied to the measured volume to include the water adhering to the inside of the test section. An electrical circuit was used to ensure

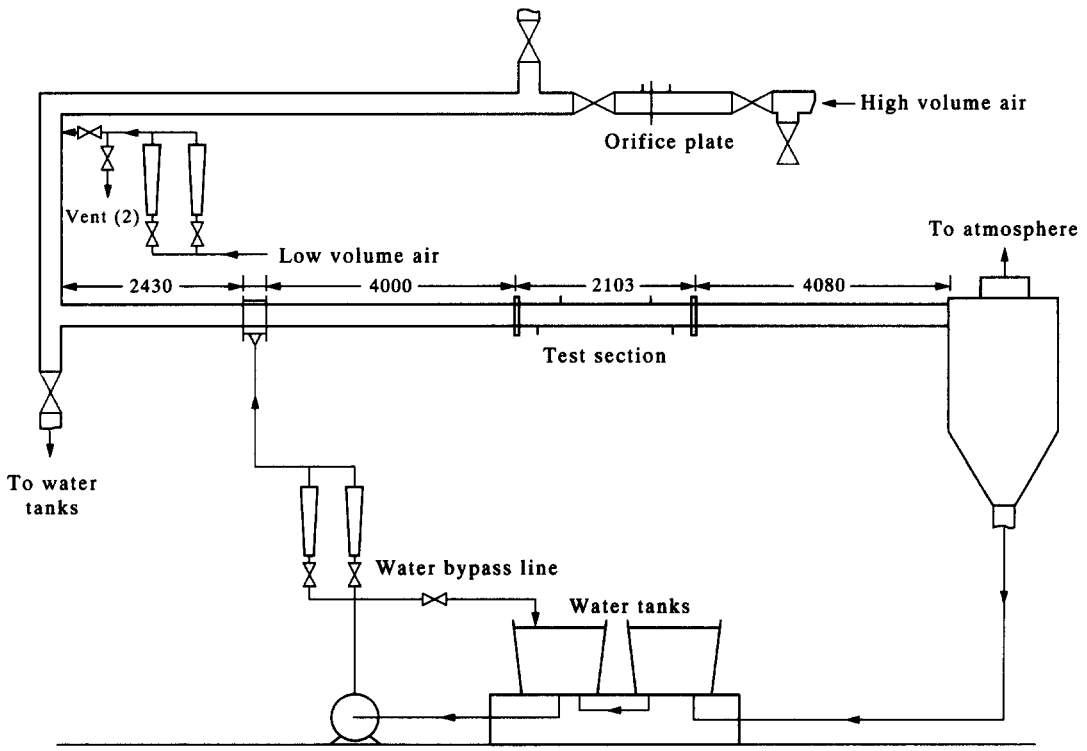

Figure 1. Schematic diagram of the experimental air–water apparatus; $d = 0.0935$ m i.d.

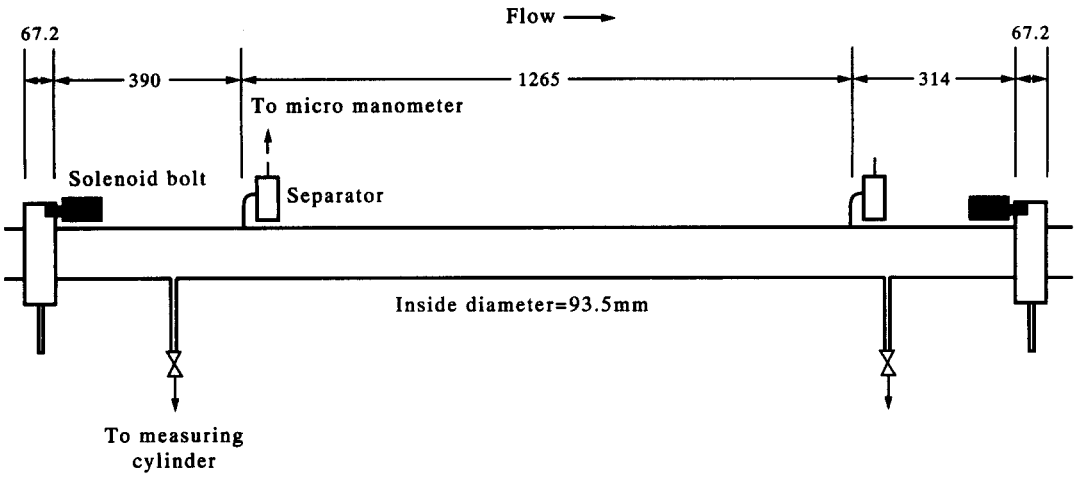

Figure 2. Schematic diagram of the test section of the experimental apparatus.

that the valves were triggered and acted simultaneously. The spring-activated sliding gates of the two valves were held in the open position using solenoids. The solenoids and the pump were electrically operated through relays which allowed the water circulating pump to be stopped 0.3 s after the valves had closed. The air was bypassed manually using a vent valve on the air line.

A great deal of care was taken to ensure the pressure tappings mounted on the top of the pipe surface were free from burrs and flush with the pipe surface. The pressure tappings were connected to small gas–liquid separators which ensured no droplets entered the pressure measuring lines.

Lighting was provided over the test section so that flow regimes could be both visually observed and recorded on video tape. An arrangement was included that allowed the recording to be linked to pressure, time and wave height data.

The apparatus was levelled accurately and care was taken to eliminate extraneous disturbances of the flow in the test section. The apparatus was checked against single-phase gas and liquid flow using the Churchill (1977) equation. The settling length prior to the test section was found to be sufficient for the development of the flow regimes observed. However, certain other flow regime data, particularly in the slug (S) pattern, required a longer time/length to develop than would be obtained in this rig and were avoided. The averaging method of Brill *et al.* (1981) was employed to handle any intermittency in the recorded data. Data are presented in Spedding *et al.* (1989).

Flow Patterns

Flow pattern recognition

A number of different methods have been proposed for the recognition of flow patterns ranging form visual observation to characteristic fluctuations in holdup, conductivity and pressure that "fingerprint" the particular patterns (cf. Dukler & Hubbard 1975; Weisman *et al.* 1979; Hewitt 1982; Barnea & Taitel 1986; Lin & Hanratty 1987b). The flow regimes in this work were identified by using a combination of techniques, viz. visual/video observations, pressure fluctuation characteristics and a detailed examination of pressure loss and holdup data. The former method is self-evident. In the latter case the data were plotted in a number of ways not only to show consistency of the actual measurements but to identify any changes characteristic of a flow pattern change. For example, in figure 3 the holdup data for a liquid volumetric rate $Q_L = 0.01\ m^3\ min^{-1}$ (corresponding to a liquid superficial velocity $\bar{V}_{SL} = 0.0968\ m\ s^{-1}$) show a general consistent trend, with perhaps the exception of the data point at a gas volumetric rate $Q_G \simeq 0.03\ m^3\ s^{-1}$. Here the data were slightly above the general trend. Repeat determinations gave it to be more correctly placed on the line. In addition the inflection at $Q_G < 0.02\ m^3\ s^{-1}$ was characteristic of the formation of a crescent shape to the interface at the onset of the stratified plus ripple (St + R) regime.

The trends that emerged from figrue 3 were that as Q_L increased the range of the stratified (St) and St + R flow patterns constricted, while the range of the stratified plus roll wave (St + RW) and film plus droplet (F + D) flows expanded. Further, as Q_G increased, increasing shear between the

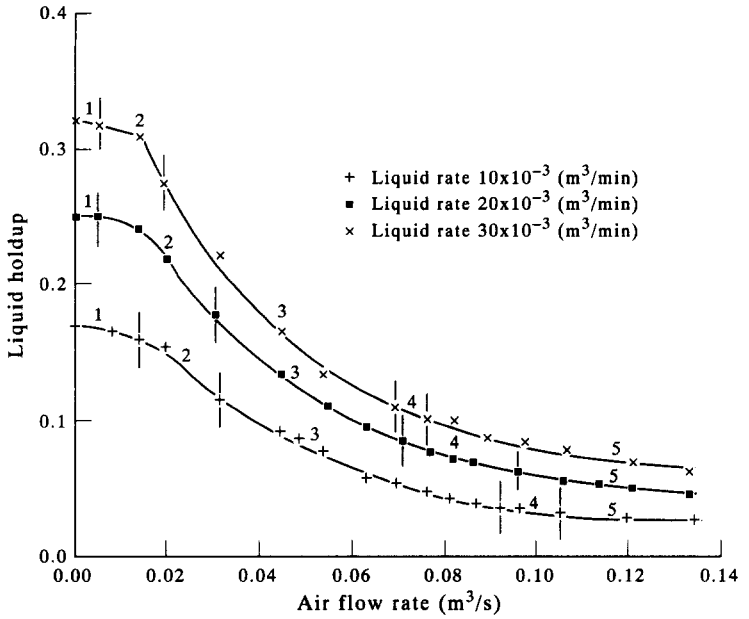

Figure 3. The effect of increasing gas flow rate on the liquid holdup for various set liquid rates.

fluids caused the interface to become more disturbed and the holdup dropped as more liquid was entrained.

Flow pattern transitions have been followed by analysing holdup fluctuations (cf. Jones & Zuber 1975; Barnea *et al.* 1980a; Vince & Lahey 1982; Geraets & Borst 1988). The method is possible when holdup is measured by beam attenuation or conductance but in this work with the quick-closing valves which, while giving more reproducible results, tended to give data that were averaged over time and space to a greater extent, thus effectively ameliorating any fluctuations.

Pressure loss fluctuations proved to be a useful adjunct to other methods in determining flow regimes and their transitions. The same principle was employed by Annunziato & Girardi (1985, 1986), who found that studying both the void fraction and pressure loss fluctuations together gave a superior indication of the flow pattern.

Figure 4 shows the effect on pressure loss fluctuations of increasing the gas flow rate for set liquid conditions of $\bar{V}_{SL} = 0.0485$ m s^{-1} and an initial liquid-only flow holdup of $\bar{R}_{LO} = 0.25$, i.e. the initial liquid level in the pipe was below the pipe centre. The pressure loss fluctuations observed increased with increasing gas rate due to waves being formed, which led to an increase in interfacial roughness and droplet formation.

The first two flow patterns encountered, namely the St and the St + R regimes, had little effect on pressure loss fluctuations. Discernible features on the pressure loss trace only became apparent with the onset of the St + W pattern, after which the range of fluctuations increased steadily with the superficial gas velocity ($\bar{V}_{SG}$) up to a plateau at the onset of the droplet (D) regime formation. Thereafter, the statistical pattern and shape of the fluctuations altered. In general, the peaks and troughs became more pronounced and sharper in form, while the pressure loss fluctuation range began to increase once more in a regular fashion until the annular (A) regime was formed where the range of the fluctuations was large.

The pressure loss traces collected over a 2 min period were used in determining the average pressure loss using the method of Brill *et al.* (1981). For all the traces shown in figure 4 the pressure loss fluctuations were symmetrical around the average pressure loss.

If the initial liquid level, $\bar{R}_{LO}$, was fractionally under 0.5 a different set of patterns were in evidence. Figure 5 presents typical pressure loss fluctuations for $\bar{V}_{SL} = 0.121$ m s^{-1} and $\bar{R}_{LO} = 0.46$. In general, the range of the pressure loss fluctuations was greater than in the case of figure 4. The patterns showed basically the same effect when passing from the St + R to the St + RW regime. However, when $\bar{V}_{SG} = 6.38$ m s^{-1} the flow pattern changed to stratified plus large roll wave and droplet (St + LRW + D). The large roll waves showed up as identifiable peaks on the pressure loss

trace, which were no longer symmetrical around the average pressure loss. A further increase in the gas flow rate caused the large roll waves to cease and their characteristic peaks disappeared from the pressure loss trace. The reason being that the increased gas flow rate caused the average liquid depth to be depressed to such an extent that the large roll waves could no longer be supported. This led to the stratified plus roll wave and droplet (St + RW + D) flow pattern, where the pressure loss fluctuations were less and were symmetrical around the average pressure loss value. Again, the characteristic sharp peaks associated with droplet formation were noted for the St + LRW + D and St + RW + D regimes. Increasing the gas flow rate further led to the formation of the F + D flow pattern and a steady increase in the magnitude of the pressure loss fluctuations

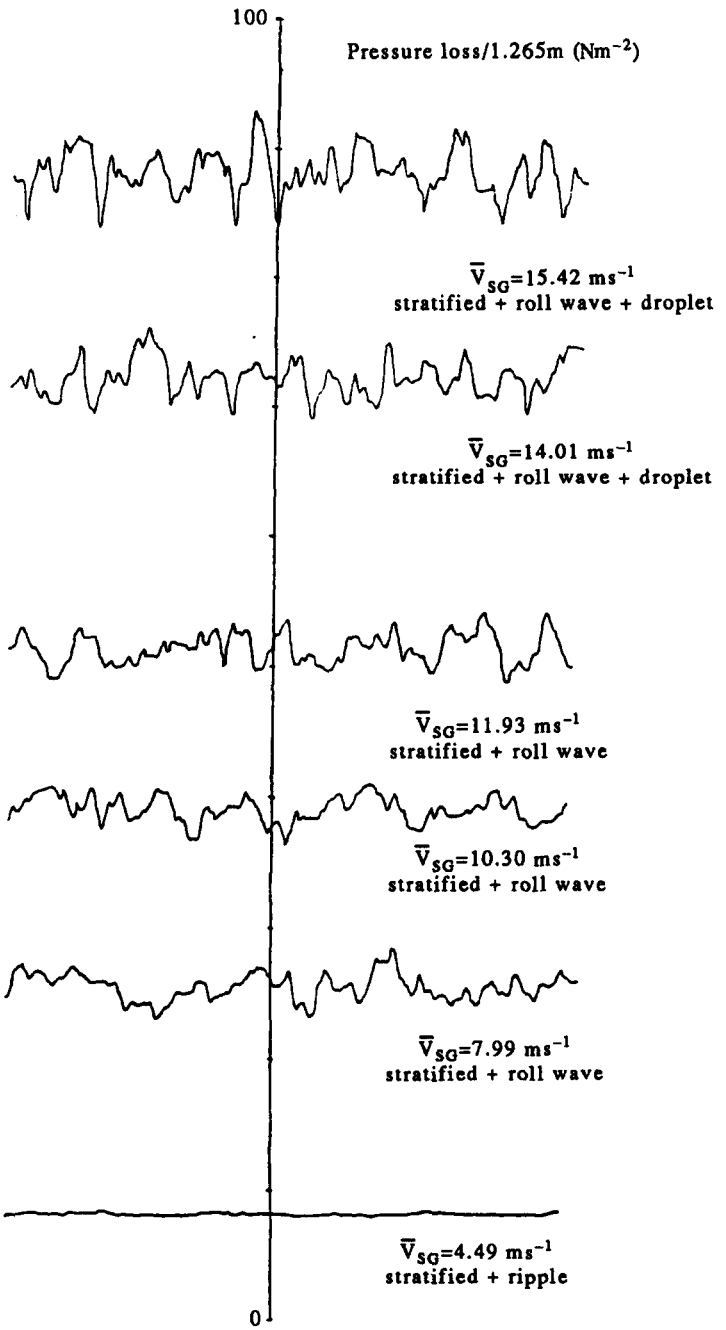

Figure 4. Flow regimes and pressure loss fluctuations over the 1.265 m test section. Conditions: $\bar{V}_{SL} = 0.0485\,m\,s^{-1}$, $\bar{R}_{LO} = 0.25$, chart speed = 240 mm min^{-1}.

due to increased droplet entrainment and liquid surface roughness. The F + D regime possessed the sharp peak characteristic of droplet formation, with the pressure loss fluctuations being symmetrical about the average pressure loss.

When $\bar{R}_{LO}$ was increased beyond 0.5, as in figure 6 for $\bar{V}_{SL} = 0.169$ m s^{-1} and $\bar{R}_{LO} = 0.575$, the stratified plus inertial wave (St + IW) flow pattern appeared. This type of flow was characterized by a liquid turbulence dominated swell wave which had no significant effect on the pressure fluctuations. As the gas flow rate was increased further the S flow pattern was first encountered, then the stratified plus blow through slug (St + BTS) and the F + D patterns.

Figure 7, for $\bar{V}_{SG} = 2.824$ m s^{-1}, shows a typical trace of the static pressure variations at the upstream tapping for S flow. From point 1 to point 2 the static pressure in the pipe rose, being indicative of the pipe filling with water up to a level where slugging could be initiated. At point

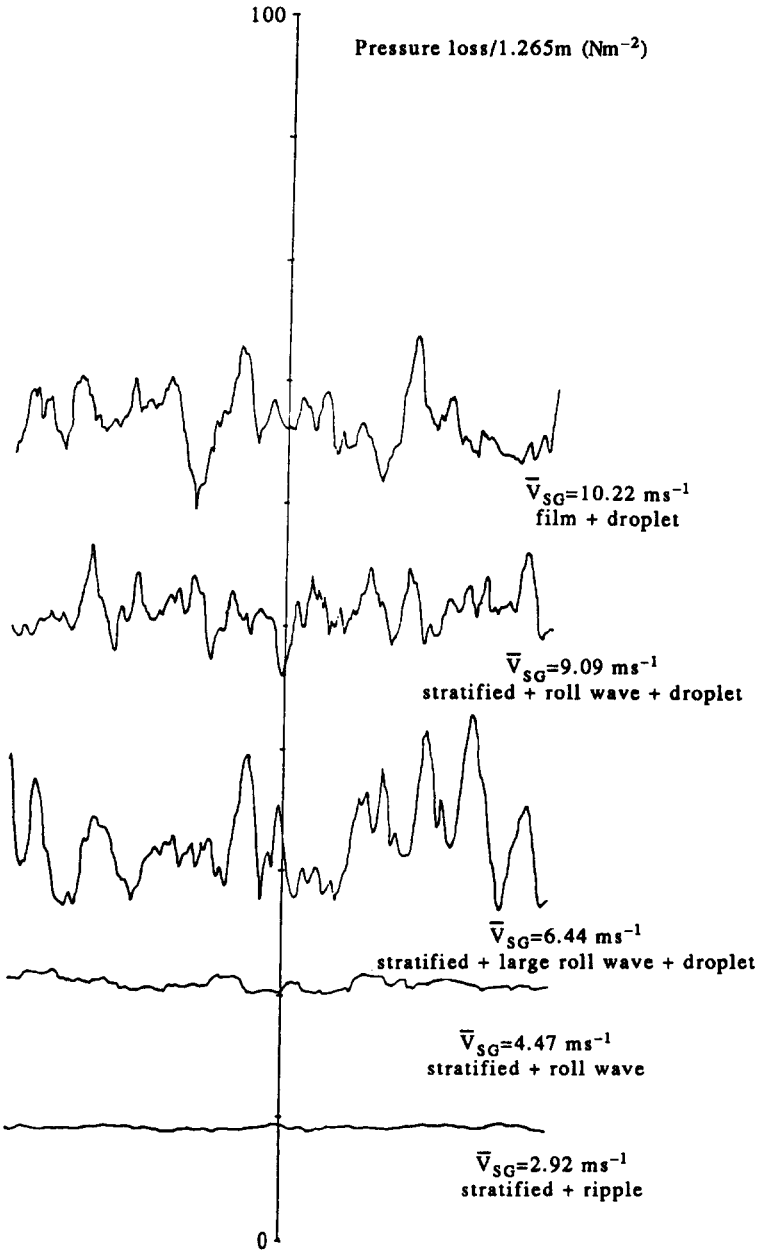

Figure 5. Flow regimes and pressure loss fluctuations over the 1.265 m test section. Conditions: $\bar{V}_{SL} = 0.121$ m s^{-1}, $\bar{R}_{LO} = 0.46$, chart speed = 240 mm min^{-1}.

3 a small surge wave passed down the pipeline. On exiting the line the surge wave induced a liquid slug, indicated by the large peak at point 4. Visual observations suggested that the liquid slug produced had the characteristic front, body and tail expected for a normal slug. The slug indicated at point 4 originated downstream of the mixing section. After the slug had exited from the pipeline, two waves, caused by the pipe refilling with water, moved in both the upstream and downstream directions from the mixing section. Since the slug shown at point 4 had originated downstream of the mixing section, the liquid level upstream of the mixing section had been relatively unchange. The increase in liquid height due to the wave was sufficient to cause another liquid slug to be induced upstream of the mixing section. Visual observations confirmed that the slug produced was shorter and more frothy in nature than that produced previously and indicated at point 4. The slug began to dissipate when it reached the downstream side of the mixing section due to the lower water

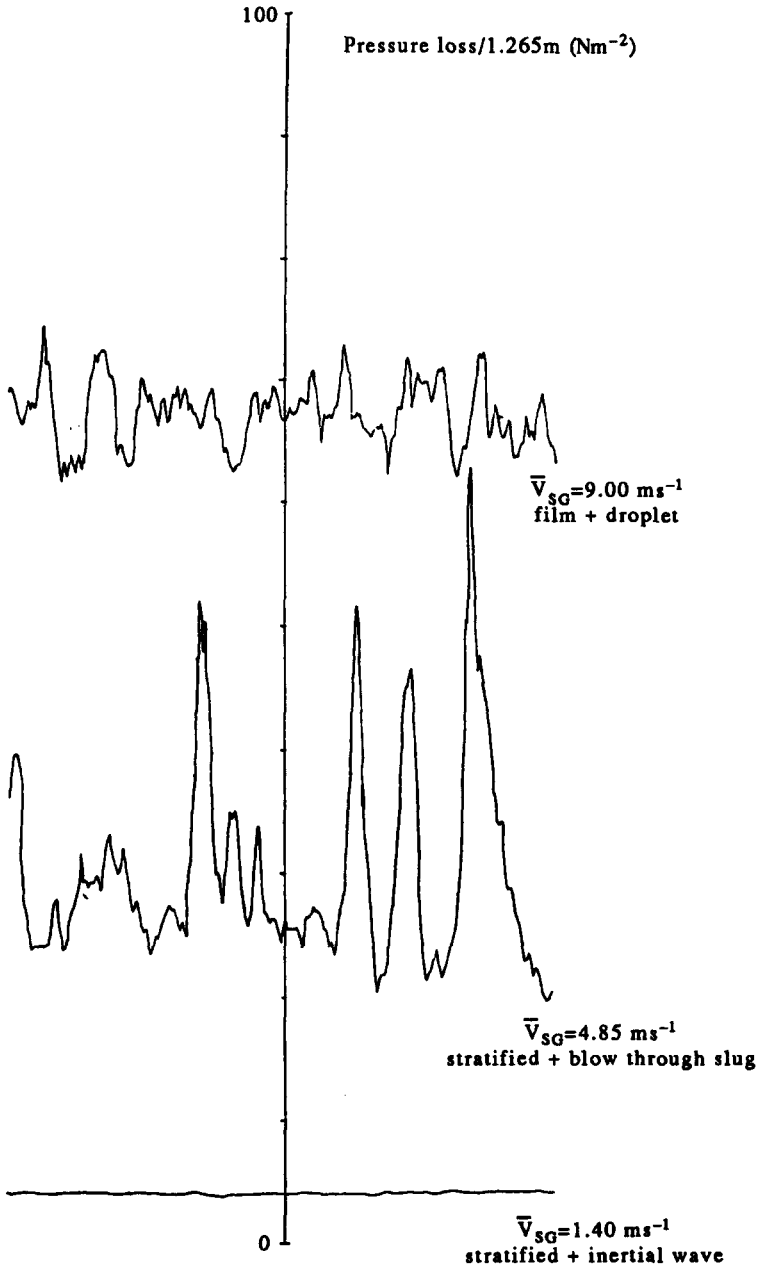

Figure 6. Flow regimes and pressure loss fluctuations over the 1.265 m test section. Conditions: $\bar{V}_{SL} = 0.169\ \text{m s}^{-1}$, $R_{LO} = 0.575$, chart speed = 240 mm min^{-1}.

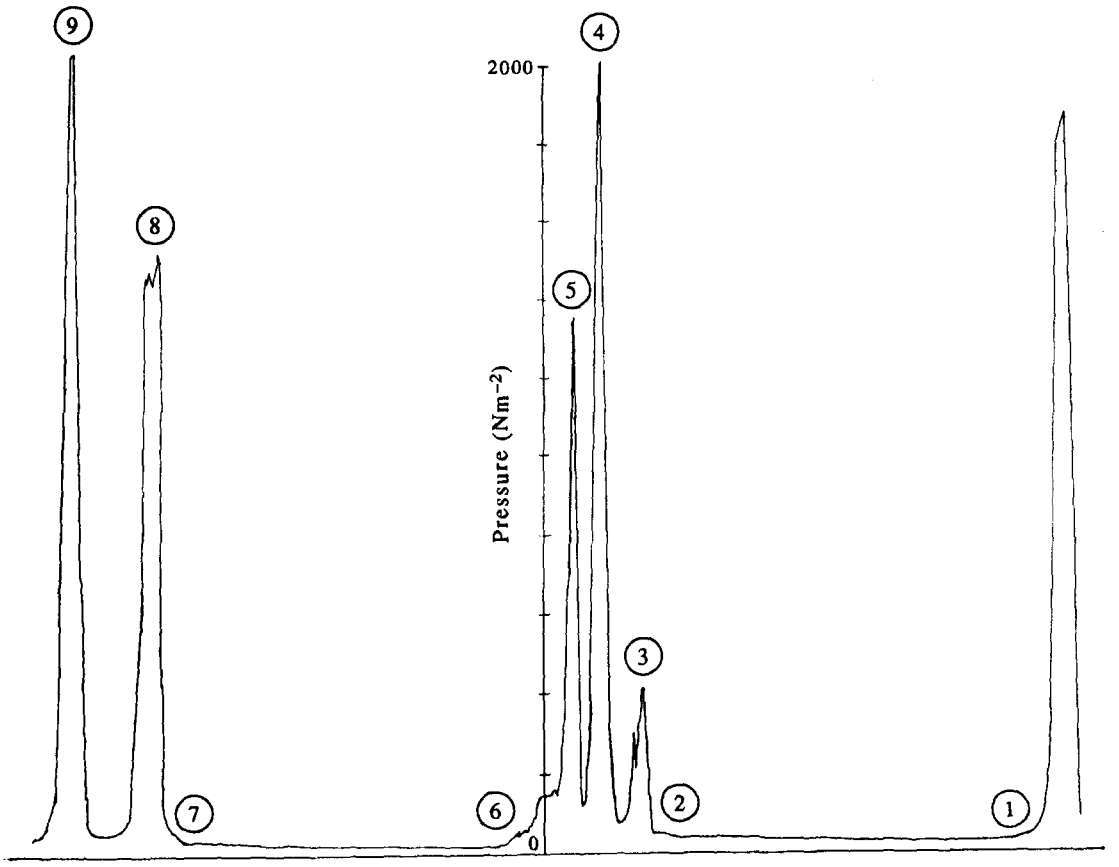

Figure 7. Pressure fluctuations for slug flow compared with atmospheric pressure. Conditions: $\bar{V}_{SG} = 2.824$ m s^{-1}, $\bar{V}_{SL} = 0.14$ m s^{-1}, chart speed = 240 mm min^{-1}.

level present at that point and resulted in a lower pressure fluctuation at point 5. Between points 6 and 7 the liquid level began to build up again and a short frothy slug was produced at point 8. Again, on exiting the pipeline another slug was induced at point 9 commencing a repeat of the cycle. The effect of another slug being induced by the exit of the previous slug had also been observed by Fairhurst (1988) and Ruder *et al.* (1989).

A further increase in the gas rate caused the transition from S to St + BTS flow. This latter flow pattern was composed of short frothy pulses. A typical pressure loss trace for St + BTS flow is shown for $\bar{V}_{SG} = 4.85$ m s^{-1} in figure 6. The pattern was characterized by large frequent peaks which were much greater than those observed for the St + LRW + D flow patterns but smaller than those for S flow. A further increase in the gas flow rate led to the F + D flow pattern.

The liquid holdup, $\bar{R}_{LFS}$, just before slugging occurred, ranged from 0.25 to 0.68 for both the S and the St + BTS flow patterns. This was in keeping with the experimental observations of Crowley *et al.* (1985), Jepson (1987) and Ruder *et al.* (1989), who suggested that $\bar{R}_{LFS}$ should have values >0.2. In general, for each value of $\bar{V}_{SL}$, the first liquid slug occurred when $\bar{R}_{LFS} > 0.5$, whereas for the St + BTS pattern the value of $\bar{R}_{LFS}$ ranged from 0.25 to 0.35. The spread of $\bar{R}_{LFS}$ values was very large, e.g. +150 to −45%, indicating that large liquid slugs were being formed. At higher $\bar{V}_{SG}$ values the spread was reduced, e.g. ±15%, as shorter more frequent slugs were being formed. Further, for S flow the spread of $\bar{R}_{LFS}$ was not evenly distributed around the mean value. By contrast with the St + BTS regime the spread of $\bar{R}_{LFS}$ values became much smaller ($> \pm 10\%$) and more evenly distributed around the mean value. However, the spread was much larger than that observed for the separated flow patterns, where values ranged from ±1 to 2%. The pressure loss fluctuations for the annular plus roll wave (A + RW) pattern are compared with those for F + D flow in figure 8 where $\bar{V}_{SL} = 0.242$ m s^{-1} and $\bar{R}_{LO} = 0.823$. The pressure loss for A + RW

flow was characterized by a series of sharp peaks that occurred with greater frequency than for the F + D flow pattern.

It is clear from this work that the static pressure variations and pressure loss data allied to video/visual and holdup observations were useful in determining flow patterns and their transitions.

Flow pattern occurrence and description

The patterns of flow developed within the conduit depended on the flow rates of the two phases and the height of the liquid initially present in the pipe. The observed flow patterns are shown in figure 9.

For a constant liquid flow with an initial level below the centreline of the pipe, the first flow pattern encountered on a systematic increase of the gas rate was the St pattern. This regime was

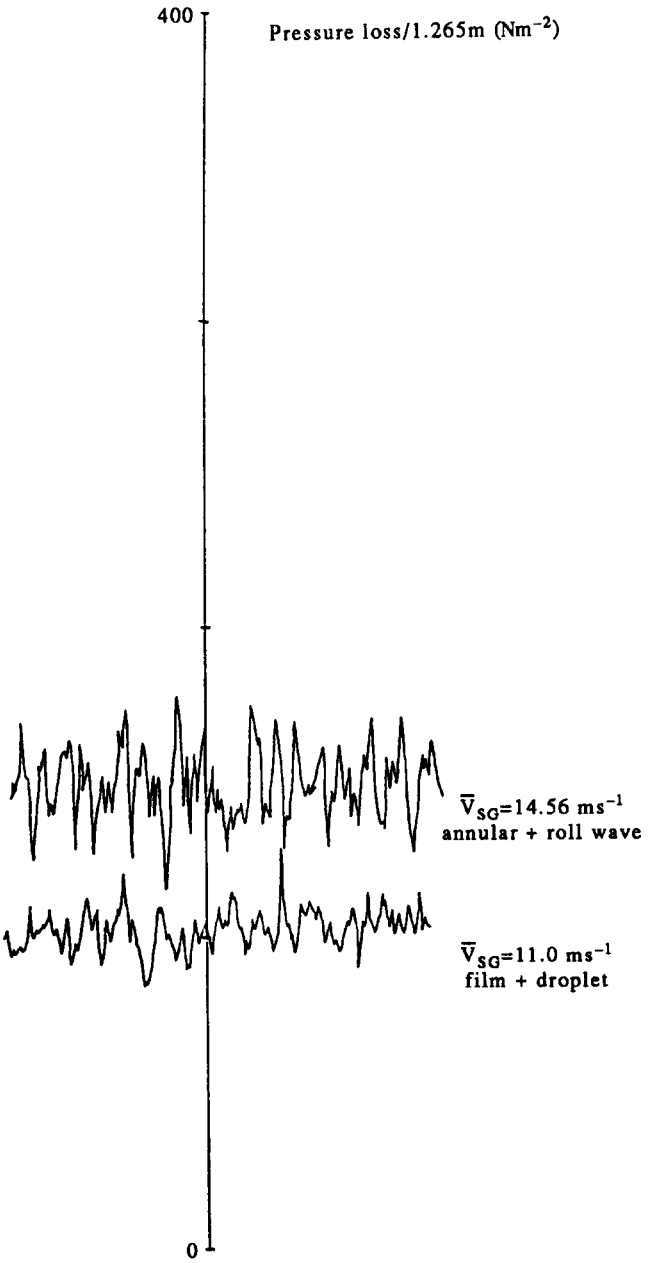

Figure 8. Flow regimes and pressure loss fluctuations over the 1.265 m test section. Conditions: $\bar{V}_{SL} = 0.242$ m s^{-1}, $R_{LO} = 0.823$, chart speed = 240 mm min^{-1}.

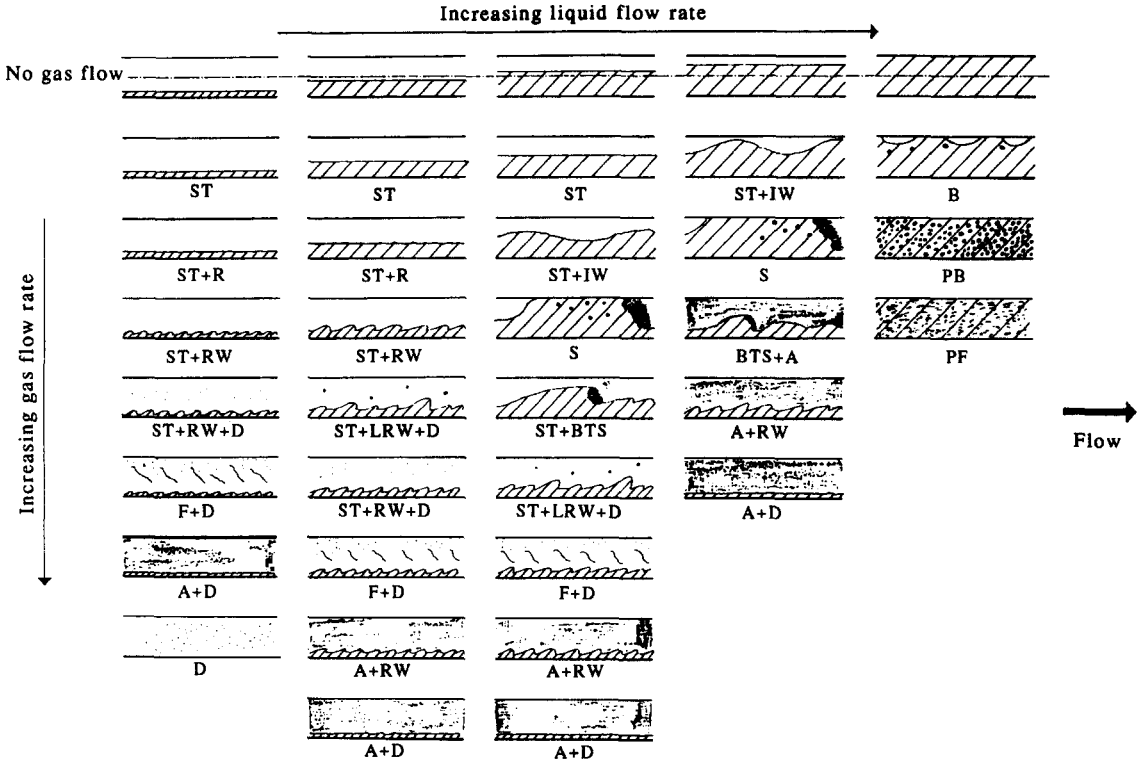

Figure 9. Observed flow patterns for a 0.0935 m i.d. pipe.

characterized by quiescently flowing liquid travelling along the base of the pipe while the gas passed over the smooth interface. It was sometimes accompanied by an interfacial liquid gradient along the length of the pipeline, particularly at low gas flow rates. Bishop & Deshpande (1986) suggested that the presence of an interfacial liquid gradient arose because the liquid phase was flowing independently of the gas phase giving liquid motion similar to open channel flow. The interfacial liquid gradient disappeared when the pressure loss measured in both phases was the same, i.e. the superficial liquid-to-gas pressure drop ratio,

$$X^2 = \frac{\left(\frac{dp}{dl}\right)_{SL}}{\left(\frac{dp}{dl}\right)_{SG}} < 1.0.$$

The presence of an interfacial gradient is in evidence in figure 10 for the condition $Q_G < 0.014\ m^3\ s^{-1}$. A gas flow above this rate acted to first remove the interfacial liquid gradient and then to reduce the liquid level by shearing effects. Any subsequent increase in the Q_G resulted in the interface becoming disturbed and surface ripples appeared to give the St + R pattern. The ripples increased in height and complexity and eventully gave rise to the St + RW pattern. Andritsos & Hanratty (1987) described the St + R region as "two-dimensional waves" and the St + RW pattern as "large-amplitude Kelvin–Helmholtz waves". Lin & Hanratty (1987a) determined that for a pipe of 0.0953 i.d. the St + RW flow pattern was not encountered until $\bar{V}_{SG} > 5\ m\ s^{-1}$, i.e. $Q_G > 0.35\ m^3\ s^{-1}$, which is in agreement with this work.

As the gas rate was increased for these stratified flows the level of liquid in the pipe decreased (cf. figure 10), the liquid cross-section became crescent-shaped because of the gas pressure and turbulence exerted on the liquid surface spreading the film up the wall of the pipe. The waves washed along the sides of the pipe forming a wetted band of liquid along the wall above the permanent liquid level that was maintained by the intermittent passage of the wave edges. Eventually, as a result of increasing Q_G, droplets were torn from the crests of the waves and some were deposited on the dry upper side surfaces of the pipe. At first the number of droplets produced

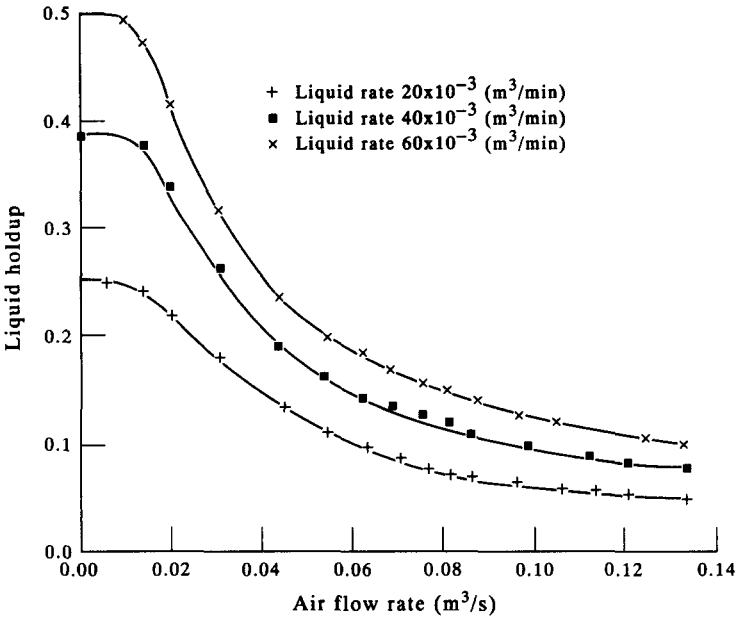

Figure 10. The effect of air flow rate on the liquid holdup for set liquid rate conditions.

was small and the top surface of the pipe was largely not wetted. Occasionally one of the droplets would impinge on the upper surface of the pipe and roll back into the liquid film, forming a rivulet on the way as it flowed down the pipe wall collecting other droplets. At this point the liquid film had not grown beyond the height of the edges of the waves. This pattern was termed St + RW + D flow.

As the gas rate was increased the liquid level was further depressed and the degree of droplet production increased. The liquid film which had previously been sustained by wave washing had now increased beyond the height of the waves and was maintained in this region by rivulets flowing down the pipe wall under the influence of gravity. Droplets were being deposited on the top of the pipe but there remained dry sections of pipe in this region. The flow pattern was termed the F + D regime. Although the St + RW + D and F + D flow patterns were very similar in nature, the important difference between them was that the mechanism for maintaining the top of the liquid film on the pipe wall was different, changing from wave washing to droplet deposition and rivulet flow, respectively.

A further increase in the gas flow rate resulted in greater atomization and the deposited film thickened and occupied a greater portion of the pipe circumference. Eventually the rivulets amalgamated and merged to form a continuous film with the onset of the A + D pattern.

As Q_G was increased the liquid layer thickness at the base of the tube became less and the eccentricity of the gas core from the pipe centre was reduced. Measurements by Sekoguchi *et al.* (1982) of the film thickness around a pipe agreed with these observations.

At very high gas velocities the liquid film around the inside of the pipe was reduced systematically in thickness towards an asympotic minimum value. Work by Armand (1946) showed a similar trend, while Dallman *et al.* (1984a,b) concluded that at high gas velocities the liquid film in A flow would decrease in thickness to the point that droplets could no longer be produced. At this particular film thickness the experimental observations suggest that the film was broken by gas turbulence and stripped from the wall to form homogeneous droplet (D) flow.

The data of Nguyen (1975) for a 0.0454 m i.d. pipe showed that Q_L was above a certain minimum value before A flow was formed. Below these conditions the transition to D flow occurred from the F + D flow pattern directly, without recourse to the A + D regime. The existence of a minimal liquid flow rate for the formation of A flow also was put forward by both Kadambi (1982) and Azzopardi & Russell (1984).

If the initial liquid level with no gas flow was slightly below the centreline of the pipe, the flow transitions described earlier applied with two exceptions. Firstly, the F + D pattern was preceded

by a new regime—the St + LRW + D, which proceeded out from the normal St + RW pattern. The St + LRW + D pattern was characterized by the production of periodic roll waves which were both greater in amplitude and velocity than the normal roll waves. These faster long roll waves were generated from the base of normal roll waves and by catching up to the normal roll waves the large roll waves began a process of wave height building through wave capture. Droplets were formed from the large roll waves and deposited on the side walls of the pipe. Frothy slugs arose by larger roll waves building upon slower-moving roll waves. This flow pattern was known as St + BTS. The frothy waves did not completely fill the pipe and were of a different nature to S flow.

The second effect observed was the occurrence of the A + RW flow pattern. This was characterized by a thin continuous film covering the pipe walls and a portion similar to St + RW flowing in the lower half of the pipe. As Q_G was increased the thickness of the wavy layer was reduced and the transition to A + D flow occurred.

If the liquid level for zero gas flow was above the centre of the pipe, a different series of flow patterns were formed. For low air flow rates the St flow pattern with the interfacial gradient still existed. A slight increase in the Q_G resulted in a long swell wave developing which was described as the St + IW flow pattern. The frequency, speed and amplitude of the inertial waves increased with the gas rate until one of these waves completely blocked the pipe, forming a liquid slug. Kordyban (1977a,b; 1985) and Kordyban & Ranov (1970) observed the same mechanism for the production of liquid slugs in a rectangular channel. Liquid holdup values measured just before slugging occurred, $\bar{R}_{LFS}$, indicated that at the transition to S flow from St flow, $\bar{R}_{LFS} > 0.5$.

The first type of slug produced had a discernible front, liquid body and tail: gas was entrained into the front of the slug and existed as discrete bubbles in the slug body. A subsequent increase in Q_G resulted in slugs becoming more frequent and also a great deal shorter and more frothy. Eventually, the gas forced through the body of the slug to give short frothy pulses which provided no major liquid blockage to the gas flow. This flow pattern was again St + BTS and gave a different set of characteristics to S flow.

Subsequent increases in the gas flow rate caused the transitions to the St + LRW + D, F + D, A + RW and A + D regimes. When the initial liquid rate was such that the pipe was almost completely full, the St + IW and S flow patterns were still observed to occur with increasing gas flow rate. For these conditions, however, the transition from S to A flow occurred through the annular plus blow through slug (A + BTS) pattern, formed by the gas breaking through the centre of the slugs. This flow pattern was characterized by forthy fluid with an intense wavy interface where the waves wrapped around the pipe circumference. These waves eventually became frequent enough to sustain an annular film with increasing Q_G leading to A + W and then A + D flows. When the initial water flow virtually filled the pipe the introduction of the gas caused the B flow pattern to be formed. Subsequent increases in Q_G gave rise to the plug (Pl) and froth (Fro) flow patterns.

COMPARISON OF FLOW REGIME MAPS

Spedding & Nguyen (1980) reviewed flow regime maps and identified the main criteria involved in map development, i.e. the use of mapping parameters that accurately reflected the basic regime transitions, the form of the mapping parameter used so as to eliminate gross disparity between map areas and the need for the map to handle the operational, physical and geometrical variables expected in two-phase flow.

The Baker (1954) Map

Baker (1954) developed a flow pattern map based on the experimental results of Jenkins (1947), Gazley (1948), Alves (1954) and Kosterin (1949). A substantial amount of the data was collected for 0.0254 m i.d. pipes, except for the limited 0.1 m i.d. pipe data of Kosterin (1949). The mapping parameters included two correction factors,

$$\lambda = \left[\left(\frac{\rho_G}{\rho_A}\right)\right]\left(\frac{\rho_L}{\rho_W}\right)\Bigg]^{1/2} \text{ and } \psi = \left[\left(\frac{\mu_L}{\mu_W}\right)\left(\frac{\rho_W}{\rho_L}\right)^2\right]^{1/3}\left(\frac{\sigma_W}{\sigma_L}\right),$$

to adjust for the difference between the fluid properties of density (ρ), surface tension (σ) and viscosity (μ) of the air and water at atmospheric conditions.

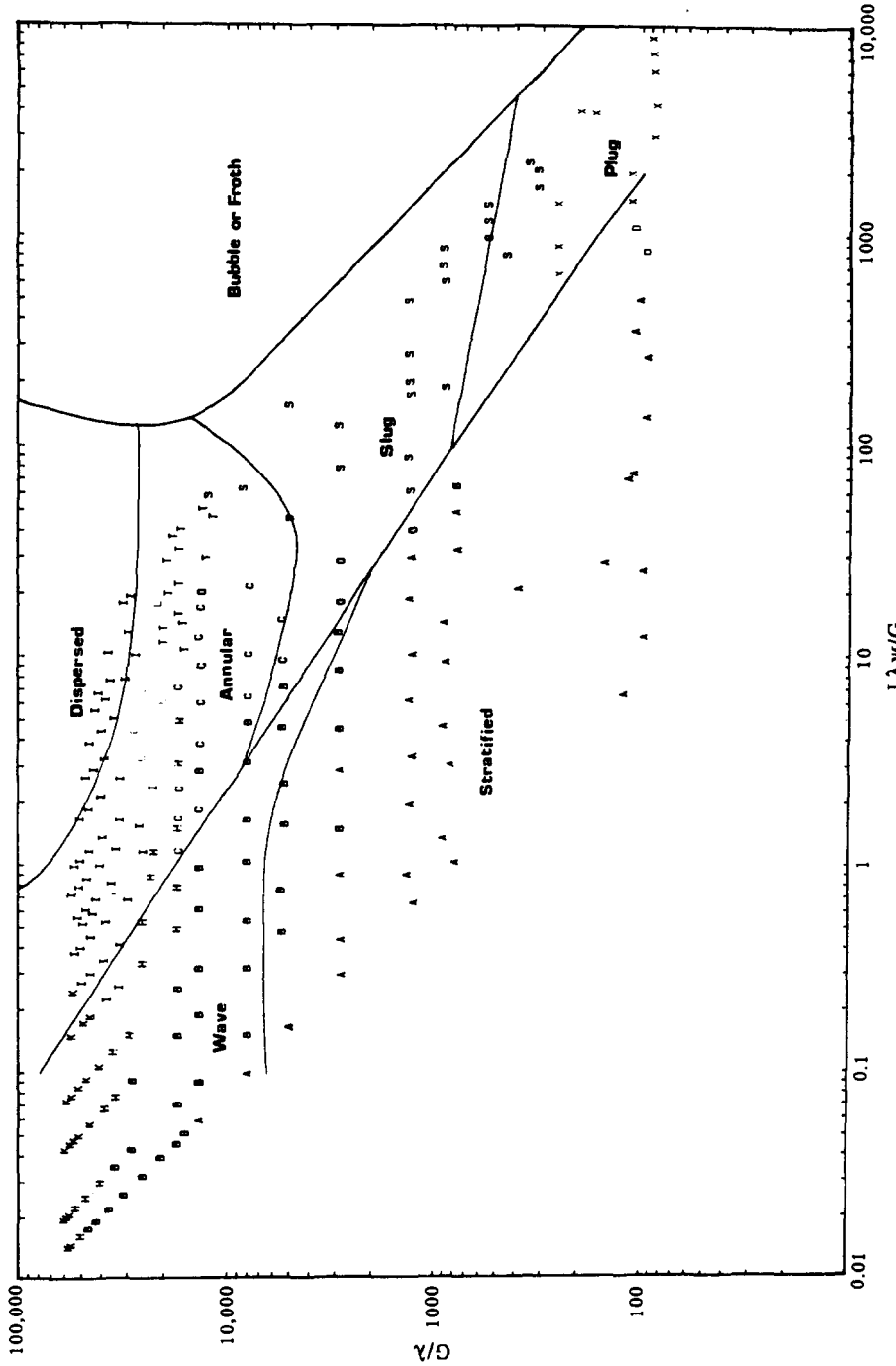

Figure 11. Comparison of the Baker air–water data of Spedding *et al.* (1989) for a pipe diameter of 0.0455 m. Symbols are detailed in the appendix.

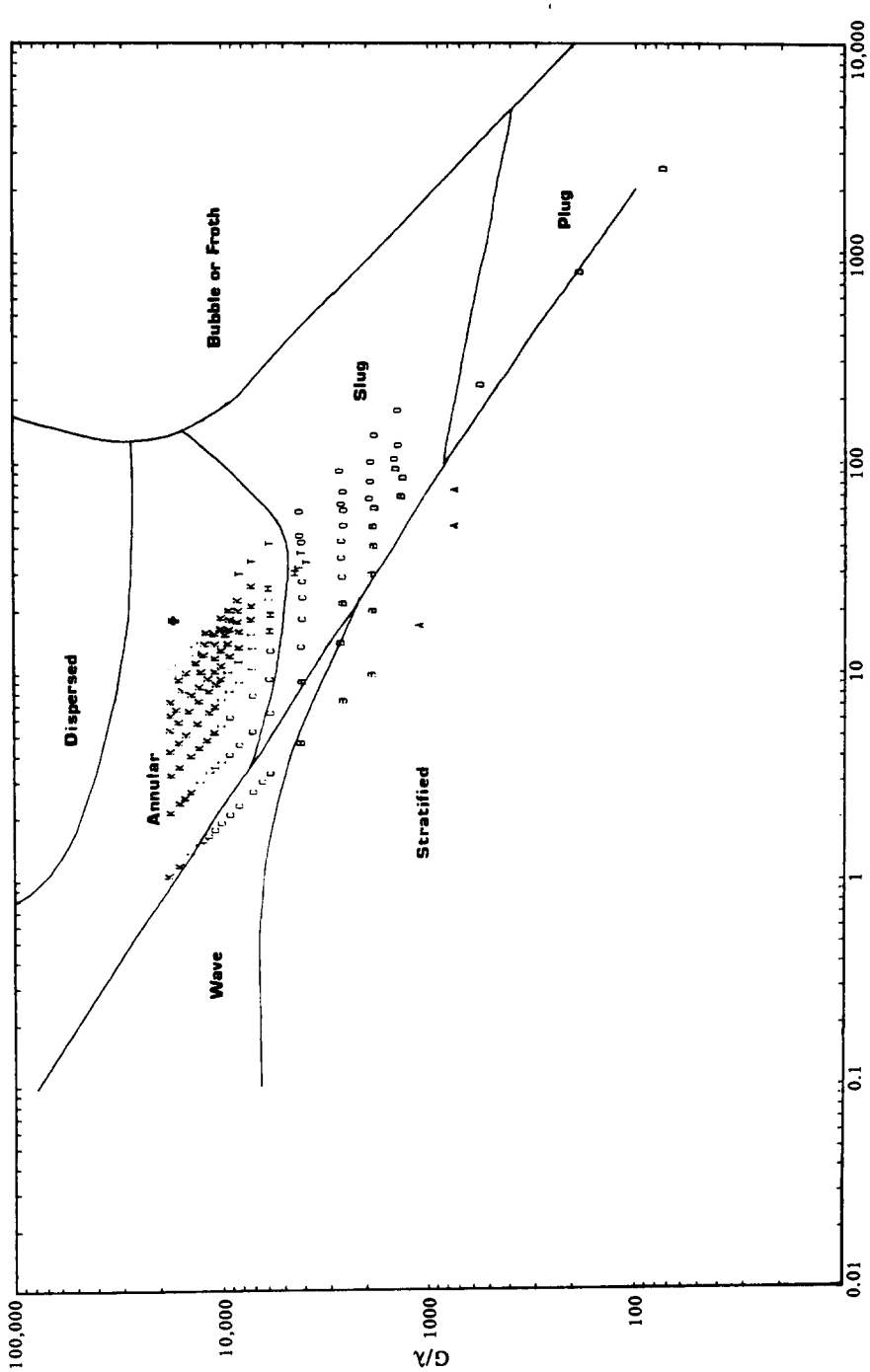

Figure 12. Comparison of the Baker (1954) flow pattern map with the air–water data of Spedding *et al.* (1989) for a pipe diameter of 0.0935 m. Symbols are detailed in the appendix.

In figures 11 and 12 the flow pattern transitions determined empirically by Baker (1954) are compared with air–water data for pipe diameters of 0.0455 and 0.0935 m, respectively. The accuracy of the map was not good for the 0.0455 m i.d. data and decreased with increasing diameter. This is to be expected, since diameter effects were not really considered. Variants by Scott (1963) and Schicht (1969) led to slight improvements but the effects of diameter could not be handled successfully.

Troniewski & Ulbrich (1984) analysed 21 flow pattern maps for horizontal gas–liquid co-current flow. They proposed the use of the Baker mapping parameters in SI units. The only variation from the Baker map was placing the bubble (B) regime below the St pattern. The reasoning behind this suggestion was that if only liquid flowed in the conduit it would fill the entire cross-section. The introduction of gas into the pipeline would result in the occurrence of B flow before leading to other flow patterns as the gas flow was increased. In figures 13 and 14 the flow pattern transitions determined by Troniewski & Ulbrich (1984) are compared to the air–water data obtained here. The map shows no significant improvement over the Baker map. In addition there was no quantitative evidence to support the B to St flow transition suggested. Indeed, it appears that the B patterns should more correctly be placed to the right of the mapping area suggested showing a B to S transition.

The Spedding & Nguyen (1980) Map

Using data collected for a co-current air–water system with a pipe diameter of 0.0455 m, Spedding & Nguyen (1980) proposed a series of empirical flow pattern maps covering angles from vertically upwards to vertically downwards.

Although Spedding & Nguyen (1980) proposed that there were some dozen different flow patterns, these were simplified into four broader classifications. Such grouping it was hoped would make flow pattern determination easier by removing some of the transitions between the more elusive patterns. After analysis of the transitions between four basic flow pattern classifications, five important variables were identified; namely, Q_L, Q_G, β, Q_L/Q_G and the Froude number, $\mathrm{Fr} = V_T/\sqrt{gd}$, where β is the volumetric dryness fraction and g is the gravitational constant. The latter two were selected as mapping parameters and to help try and equalize the areas assigned on the map to each of the four regimes, a square root logarithm form of Fr was chosen for use on the maps.

The plots presented in figures 15 and 16 have solid lines between the four pattern classifications, and dashed lines between individual flow patterns. The S, St and St + IW patterns were predicted satisfactorily but diameter effects were present for the remaining flow patterns. These observations were partially in agreement with the work of Lin & Hanratty (1987a), who showed that Fr successfully correlated with the onset of S flow and atomization but presumably not with other transitions. In addition, the effect of fluid properties could not be accounted for by the mapping parameters. The mixing theory of Ruston *et al.* (1950) formed the basis for including Fr as one of the mapping parameters, since it modelled the effect of liquid stirring while allowing the diameter to be incorporated into the relation. The map was partially successful under these conditions, so Fr only modelled mixing on the basis of turbulence injected by the movement of the liquid phase and proved to be inappropriate in cases where the gas phases provided the energy for turbulence in two-phase systems.

The Lin & Hanratty (1987b) Map

Using data collected for an air–water system in pipes of 0.0254 and 0.0953 m i.d., Lin & Hanratty (1987b) proposed the flow pattern transition map shown in figure 17. The method of map presentation used was that of Mandhane *et al.* (1974). The flow patterns in figure 17 were identified by using cross-correlation of pressure traces at two locations, conductance probe methods and visual observation. Most of the flow patterns described by Lin & Hanratty were similar in nature to the definitions given in this work. The exceptions were the wavy stratified flow, which included both the St + R, St + RW and pseudo-slug flow. The latter was considered to be formed by intermittent waves capable of wetting the entire pipe circumference without causing large pressure pulsations of the type characteristic of complete blockage of the pipe cross-section, such as in S flow. In addition, the pseudo-slug pattern did not travel at approximately the gas velocity like S flow. The pseudo-slugs were considered to be a hybrid of St, A and S flows. A thick wavy layer similar to that observed in the wavy stratified type flow pattern was present, while a continuous

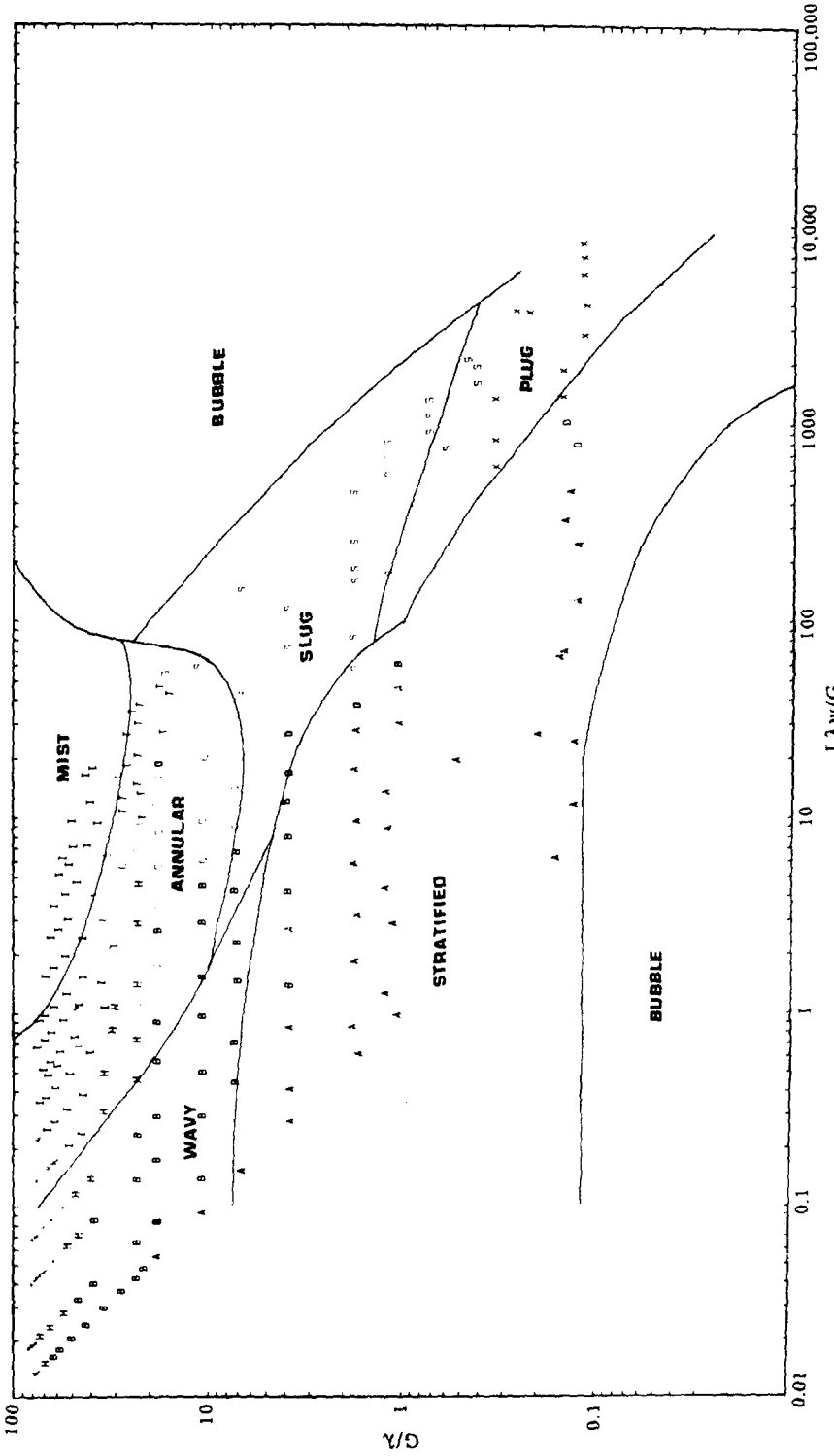

Figure 13. Comparison of the Troniewski & Ulbrich (1984) flow pattern map with the air–water data of Spedding *et al.* (1989) for a pipe diameter of 0.0454 m. Symbols are detailed in the appendix.

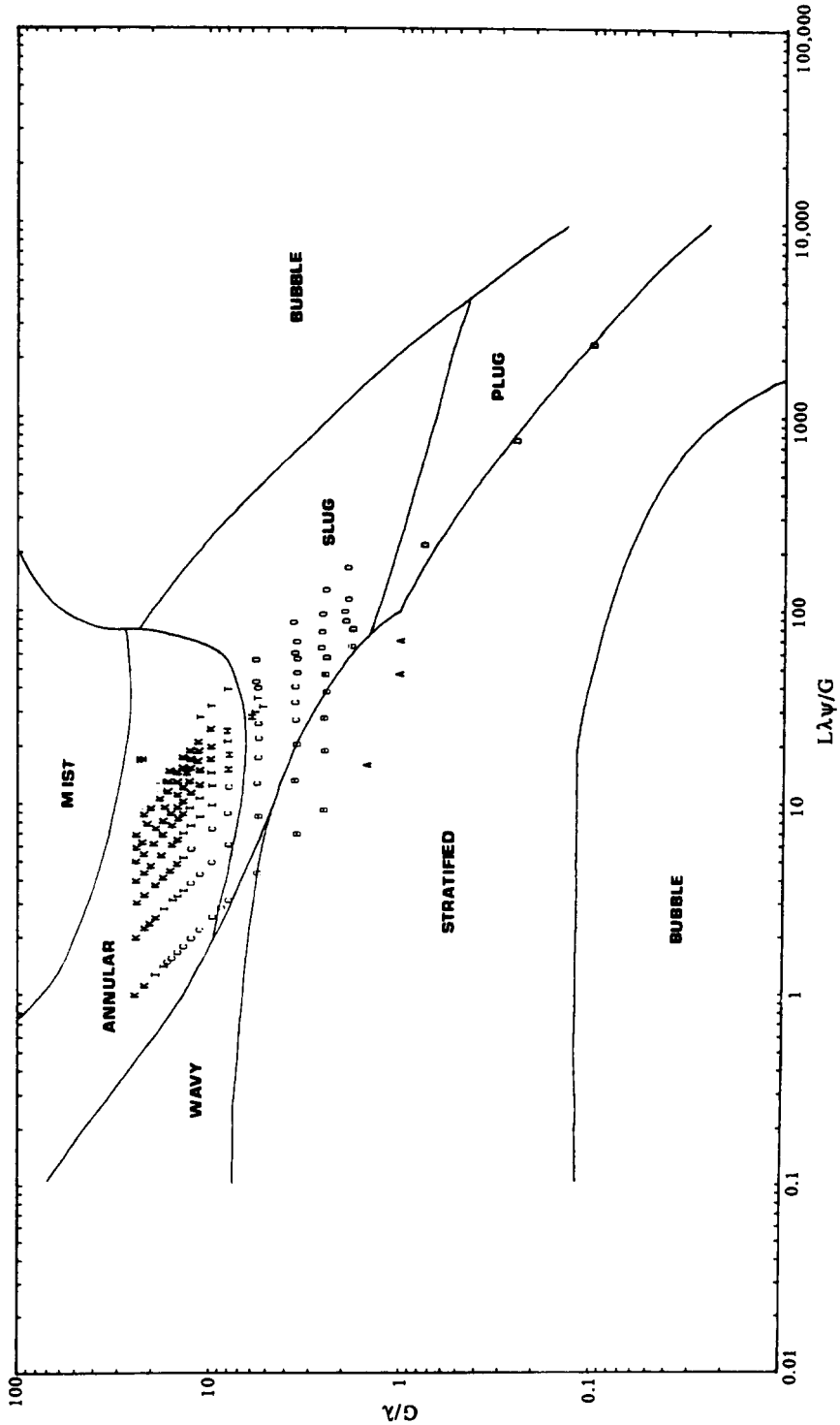

Figure 14. Comparison of the Troniewski & Ulbrich (1984) flow pattern map with the air–water data of Spedding *et al.* (1989) for a pipe diameter of 0.0935 m. Symbols are detailed in the appendix.

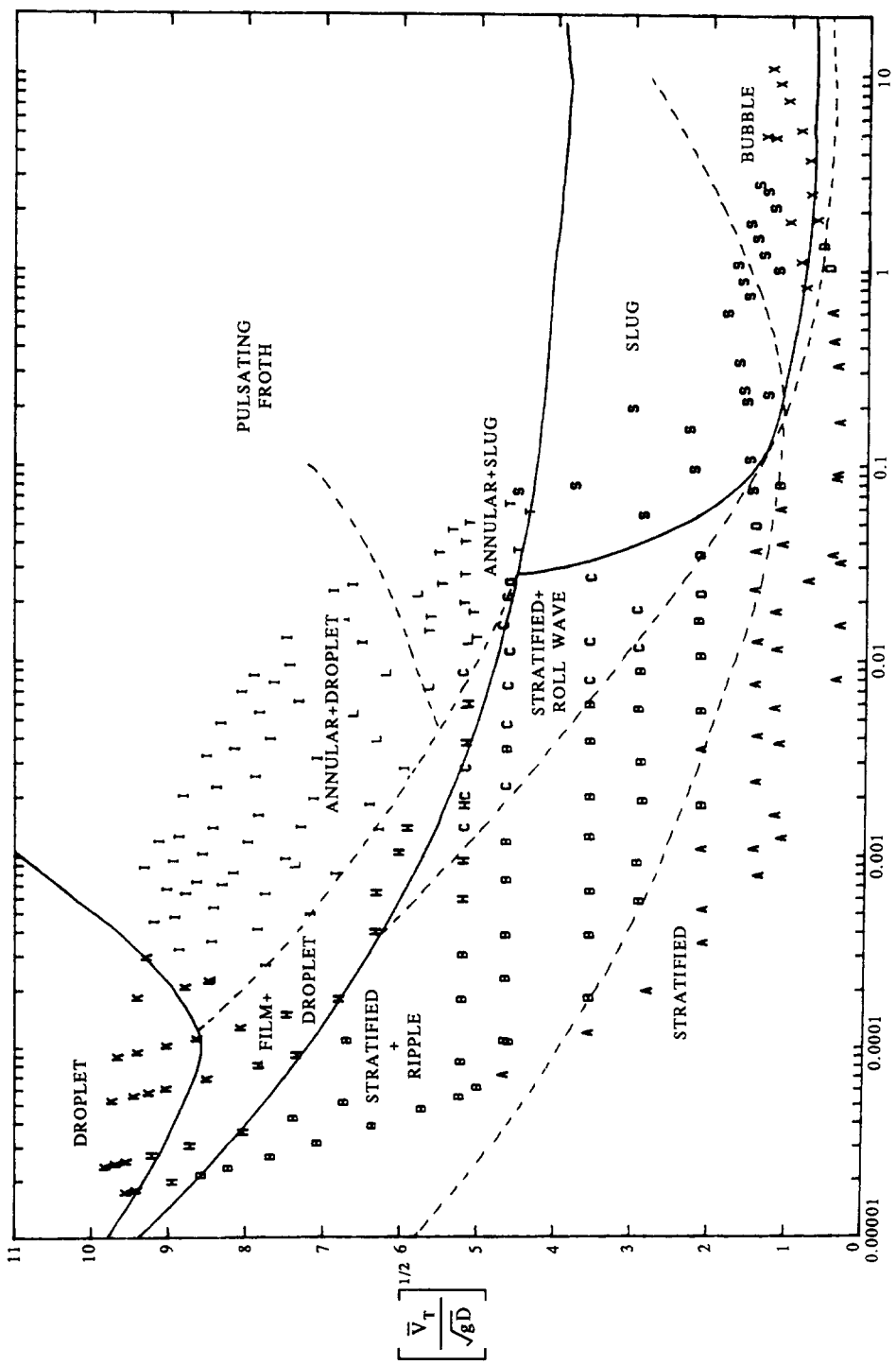

Figure 15. Comparison of the Spedding & Nguyen (1980) flow pattern map with the air–water data of Spedding *et al.* (1989) for a pipe diameter of 0.0455 m. Symbols are detailed in the appendix.

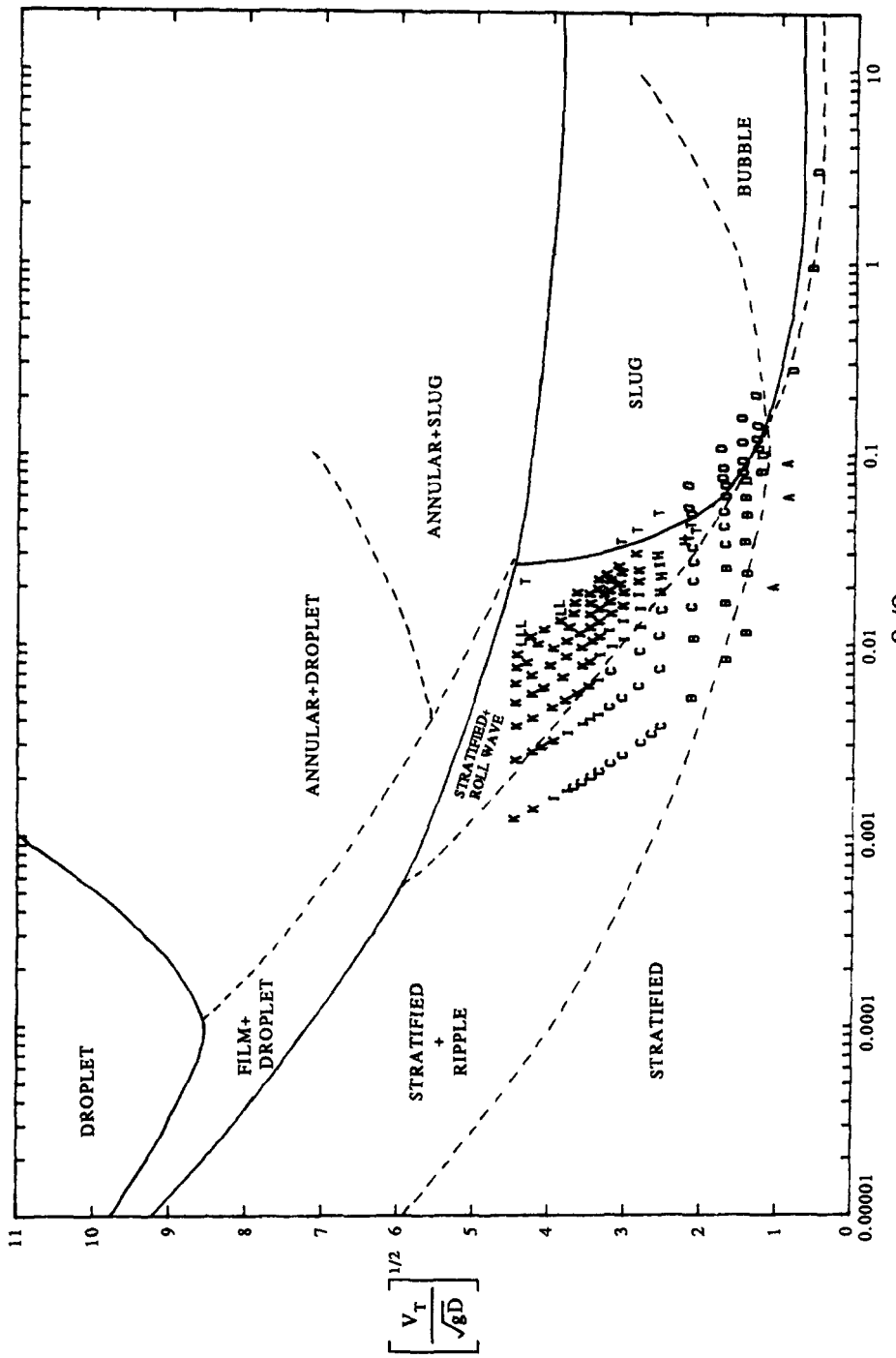

Figure 16. Comparison of the Spedding & Nguyen (1980) flow pattern map with the air–water data of Spedding *et al.* (1989) for a pipe diameter of 0.0935 m. Symbols are detailed in the appendix.

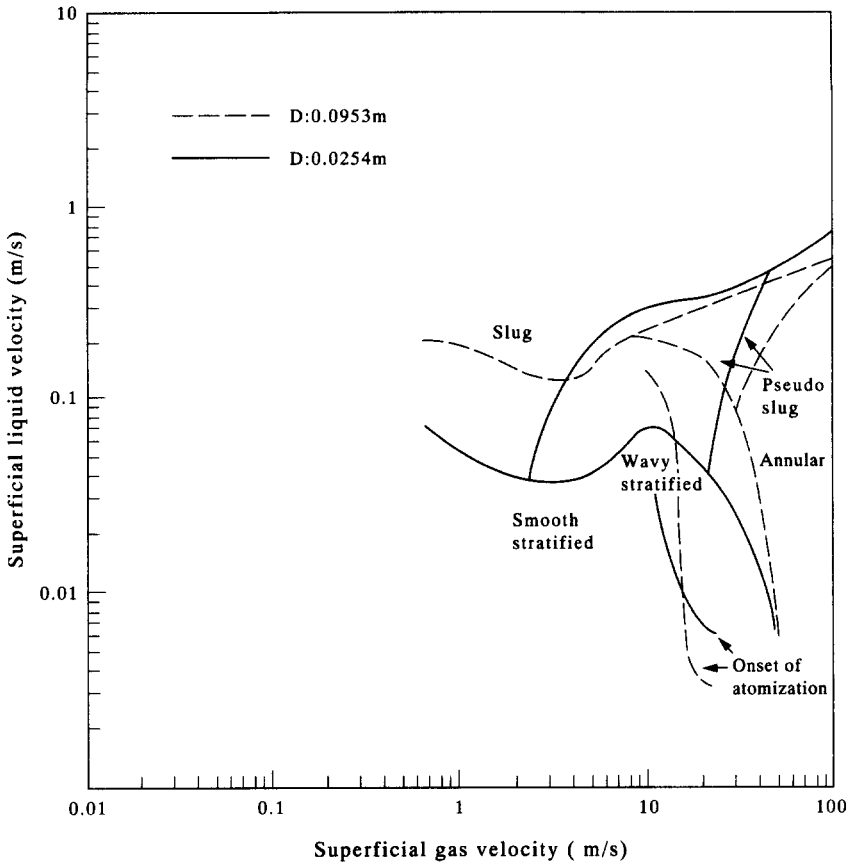

Figure 17. The proposed flow pattern map of Lin & Hanratty (1987b).

film was formed around the circumference of the pipe similar to that formed in A flow. In addition, periodic large foamy structrues, not unlike the tail end of a slug, were present. From this description the pseudo-slug pattern would include the A + BTS, St + BTS and possibly A + RW regimes mentioned in this work.

For the transition from stratified wavy type flows to S flow, two different mechanisms were noted. For low gas velocities ($\bar{V}_{SG} < 5$ m s^{-1} for the 0.0953 m i.d. pipe, $\bar{V}_{SG} < 3$ m s^{-1} for the 0.0254 m i.d. pipe), the slug transition occurred due to the Kelvin–Helmholtz type instability.

For higher gas velocities, slugs or pseudo-slugs could have occurred by the coalescence of roll waves. The production of a slug or a pseudo-slug depended upon the liquid holdup present, i.e. if there was enough liquid present to sustain a liquid slug.

Two different mechanisms were also noted for the formation of A flow. The first was the droplet production and deposition of the type studied by Hoogendoorn (1955) and Anderson & Russell (1970a,b). The mechanism was found to be effective for $\bar{V}_{SL} < 0.1$ m s^{-1} for the 0.0953 m i.d. pipe and $\bar{V}_{SL} < 0.015$ m s^{-1} for the 0.0254 m i.d. pipe. The second was the transition from pseudo-slug to A flows which occurred at larger values of $\bar{V}_{SL}$ than those already mentioned for both diameters.

After the transition from pseudo-slug to A flow had occurred, large roll waves were still present on the thicker part of the liquid film at the base of the pipe. By analysing the signals from the conductance probes it was decided that these waves could wrap completely around the pipe circumference for the 0.0254 m i.d. pipe but they were unable to do so for the 0.0953 m i.d. pipe. The wave wrapping mechanism had also been described by Butterworth (1971, 1972) and Sekoguchi *et al.* (1982), in both cases a 0.0254 m i.d. pipe was used.

From figure 17, it can be seen that the transition from stratified type flows to S flow occurred at a lower $\bar{V}_{SL}$ than for the 0.0254 m i.d. pipe; the pseudo-slug region was also expanded for the small pipe. This effect was attributed to the larger liquid interfacial height-to-diameter ratios for the 0.0254 m i.d. pipe compared with those for the 0.0953 m i.d. pipe, at similar superficial

velocities. Thus, the map was not able to accommodate changes in diameter and possibly in fluid properties.

Figure 18 shows the empirically determined flow pattern transitions for the 0.0953 m i.d. pipe compared with the 0.0935 m i.d. data collected by Spedding *et al.* (1989). The slight difference in diameter had no significant effect on the flow pattern boundaries. In general, the agreement between the map and the data was good up to $\bar{V}_{SL} = 0.1$ m s^{-1}. Thereafter, the map proved to be inaccurate for the prediction of S and pseudo-slug flows, particularly with the latter pattern which encompassed some of the F + D and all of the A + RW observations.

The transitions between St, St + R, St + RW and the onset of atomization were similar to those determined by Andritsos & Hanratty (1987). Lin & Hanratty (1987b) also presented a comparison of their experimentally determined flow pattern transition for the 0.0254 and 0.0953 m i.d. pipes with the Mandhane *et al.* (1974) map. This map was based on some 1178 flow pattern observations made for air–water systems. A facility was also provided for modifying the transition boundaries to account for fluid properties other than those of water. The overall agreement between the Mandhane plot and the Lin & Hanratty transition was poor, suggesting that the Mandhane map was particularly inaccurate in the prediction of flow patterns. Comparison between data at 0.0455 m i.d. from Spedding *et al.* (1989) and the Lin & Hanratty (1987b) map for this geometry, showed a similar situation to that described above in figure 18.

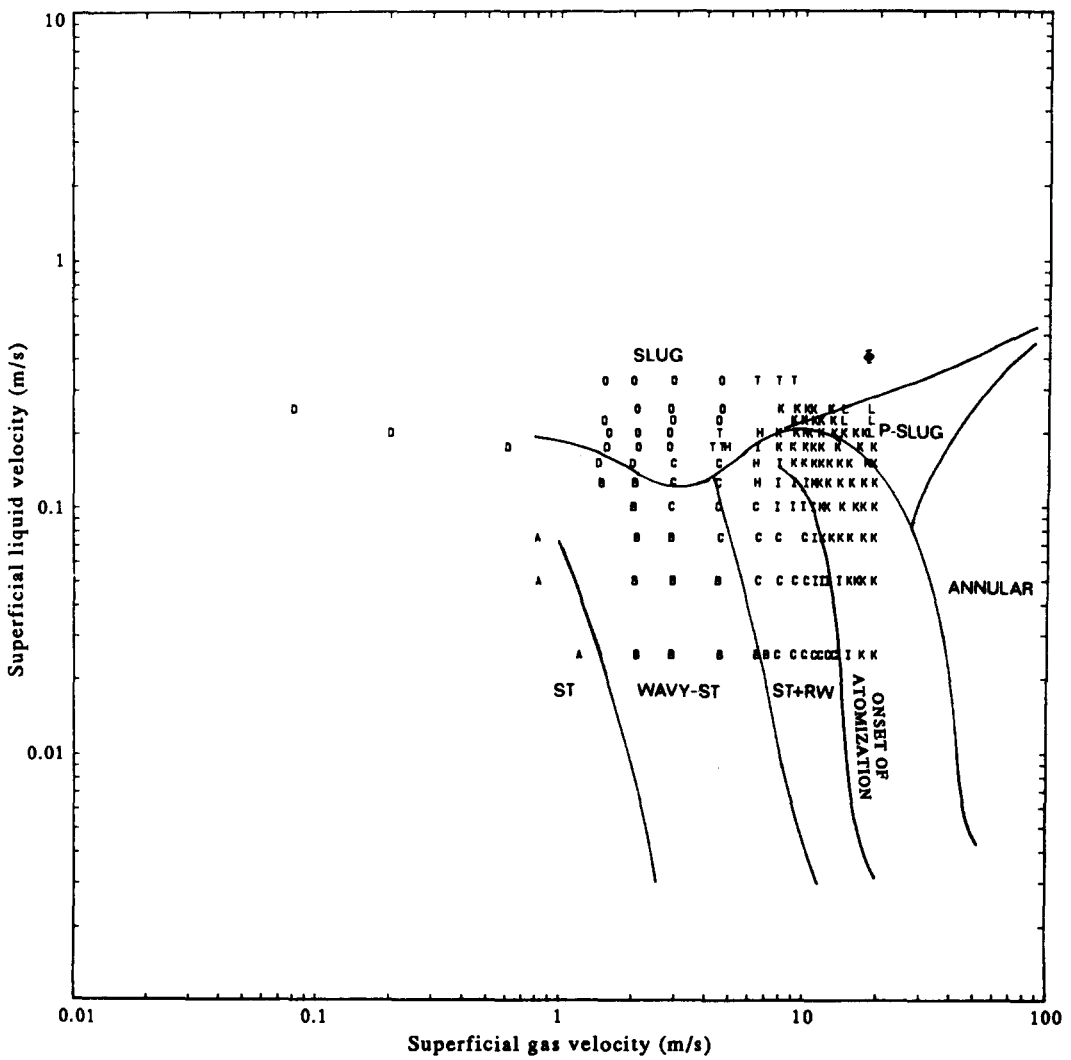

Figure 18. Comparison of the Lin & Hanratty (1987b) flow pattern map with the air–water data of Spedding *et al.* (1989) for a pipe diameter of 0.0935 m. Symbols are detailed in the appendix.

Other Maps

Of the approximately 40 maps which have been proposed for the prediction of flow regimes, tests with the data for two different diameters showed that none were successful in handling the effect of geometry and possibly the effect of changes in the physical properties of the phases. Discussion of each case would not be fruitful, since these other maps usually gave a poorer overall result than those already mentioned above.

THEORETICAL MODELS FOR THE DETERMINATION OF FLOW PATTERN

Taitel–Dukler (1976a) Model

Taitel & Dukler (1976a) developed a semi-theoretical flow transition predictive method using five dimensionless groups. The transitions were shown to be controlled by the following combination of these groups:

St to intermittent	$X,\bar{F},Y$
St to A	$X,\bar{F},Y$
Intermittent to dispersed bubble	X,T,Y
Stratified smooth to stratified wavy	X,K,Y
Intermittent to A	X,Y

where

$$\bar{F} = V_{SG}\left[\frac{\left(\frac{\rho_G}{\rho_L - \rho_G}\right)}{(dg\cos\alpha)}\right]^{0.5}.$$

α—angle of inclination,

$$T = \left[\frac{\left(\frac{dp}{dl}\right)_{SL}}{(\rho_L - \rho_G)\, g \sin\alpha}\right]^{0.5},$$

$$Y = \frac{(\rho_L - \rho_G)g\sin\alpha}{\left(\frac{dP}{dl}\right)_{SG}},$$

$$K = \bar{F}(\mathrm{Re}_{SL})^{0.5}$$

and

Re_{SL}—superficial liquid Reynolds number.

The condition of St flow was important in the predictive method. For fully developed St flow, Taitel & Dukler (1976b) used the ratio of the interfacial to superficial gas friction factor ($f_i/f_{SG} = 1.0$) to determine a relationship between X and the liquid height-to-diameter ratio (h_L/d) for the turbulent–turbulent scenario.

Barnea *et al.* (1980b) compared the transition criteria for air–water systems with pipe diameters of 0.0255 and 0.0195 m. This led to the suggestion that the agreement between the theory and the experimental data was good for angles of inclination from $\pm 10°$, but it was pointed out that the theory failed to predict the stratified smooth to stratified wavy transition for inclined pipes.

Taitel (1977) suggested that the effect of varying pipe roughness could be included into the method by using the value of f given by [1] below, where ϵ/d was the relative roughness, in the prediction of $(dP/dl)_{SL}$ and $(dP/dl)_{SG}$:

$$\frac{1}{\sqrt{f}} = 3.48 - 4\log_{10}\left[2\frac{\varepsilon}{d} + \frac{9.35}{\mathrm{Re}_{SL/SG}\sqrt{f}}\right]. \qquad [1]$$

The effect of roughness was shown to be negligible in the horizontal case for all but the intermittent dispersed bubble transition.

A modification to the theoretical transitions was proposed by Barnea *et al.* (1983) to account for surface tension effects which were suggested as an important consideration for small pipe diameters. Using data for 4 and 12 mm i.d. pipes, only the St to S transition was affected by a change in diameter and a modification to the model was proposed to account for this. It was stated that the effect of surface tension could be ignored for pipe diameters >0.025 m.

Barnea *et al.* (1982) suggested that the S to A transition should be modified to account for the gas holdup in the slug. Taitel & Dukler (1976a) suggested that the transition between S and A flows would take place at a constant value of $h_L/d = 0.5$, hence the dimensionless group X would also be constant at $X = 1.6$. Barnea *et al.* (1982) reasoned that near the S to A transition the gas holdup in the slug was 0.3, hence $\bar{R}_L = 0.7$. The transition was thought to occur when the stratified liquid holdup was half the slug holdup, therefore a value of $h_L/d = 0.35$ was used, which corresponds to an X value of 0.7. Barnea (1987) went on to propose a model for the S to A transition for the complete range of pipe inclination angles. The transition was again based on the dimensionless groups X and Y, and predicted that for horizontal flow the transition occurred at a value of $X = 1.47$.

Figures 19 and 20 show the Taitel & Dukler (1976a) transitions compared with the data from this work. For both cases the St and S transition was overpredicted. Continuation of this transition line suggested that the formation of A flow from St flow occurred at lower values of $\bar{V}_{SL}$ than those predicted experimentally.

The theoretical basis behind the flow pattern transition was the Kelvin–Helmholtz model, which provided a stability criterion for waves of infinitesimal amplitude formed on a flat sheet of liquid flowing between horizontal parallel plates.

Only the gravitational forces were considered to oppose the suction set up over the wave crest. It was determined that waves would grow provided,

$$V_G > C_2\left(\frac{(\rho_L - \rho_G)g\cos\alpha A_G}{\rho_G \dfrac{dA_L}{dh_L}}\right)^{1/2}, \qquad [2]$$

where A is the phase cross-sectional area and

$$C_2 = 1 - \frac{h_L}{d}. \qquad [3]$$

A value of $C_2 = 0.5$ was consistent with the Wallis & Dobson (1973) criteria for the onset of S flow. If $C_2 = 0.353$, then [2] described the Kordyban (1985) criteria for the transition to S flow. Equation [2] was expressed in dimensionless form as

$$\bar{F}^2\left[\frac{\dfrac{d\tilde{A}_L}{d\left(\dfrac{h_L}{d}\right)}}{\dfrac{1}{C_2^2\tilde{V}_G^2}\dfrac{}{\tilde{A}_G}}\right] \geqslant 1.0, \qquad [4]$$

where

$$\frac{d\tilde{A}_L}{d\left(\dfrac{h_L}{d}\right)} = \left\{1 - \left[2\left(\frac{h_L}{d}\right) - 1\right]\right\}^{0.5}. \qquad [5]$$

Ishii (1982) indicated that the effect of ignoring the relative motion between the fluids, the viscosities and the surface tension effects in the Taitel–Dukler analysis for the St/S transition appeared to result in the prediction of a larger stable area for St flow.

Lin & Hanratty (1986) extended the Kelvin–Helmholtz theory to include viscous and inertial terms. Their resulting transition for a 0.0935 m i.d. pipe is compared with the data for a 0.0935 m i.d. pipe in figure 20. For $\bar{V}_{SG} < 3$ m s^{-1}, the transition between St and S flow was slightly underpredicted. The criterion did, however, give a good indication of the minimum $\bar{V}_{SL}$ below which S flow could not occur. For $\bar{V}_{SG} > 3$ m s^{-1}, Lin & Hanratty (1986) suggested that the

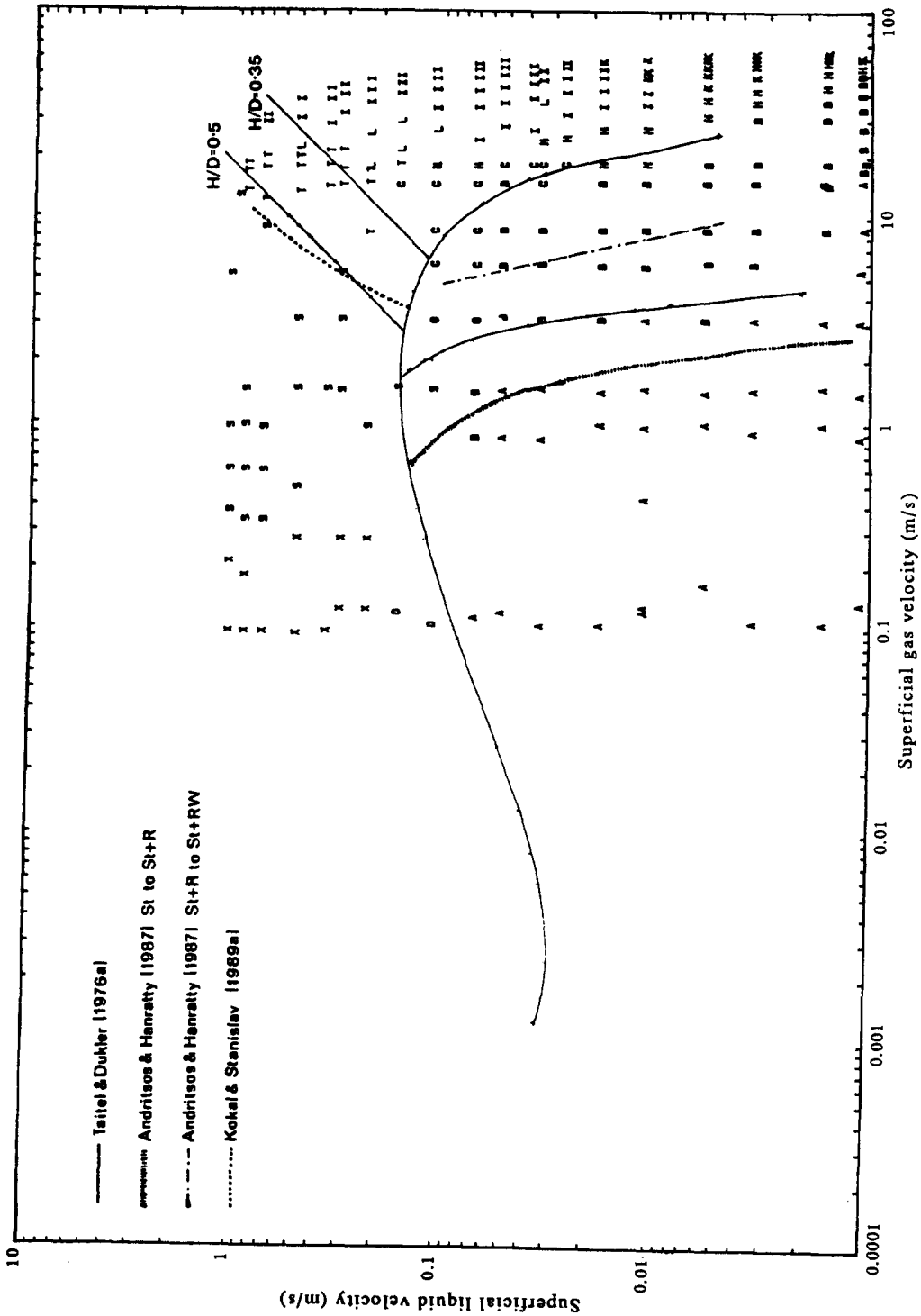

Figure 19. Comparison of theoretical flow pattern transitions with the air–water data of Spedding *et al.* (1989) for a pipe diameter of 0.0455 m. Symbols are detailed in the appendix.

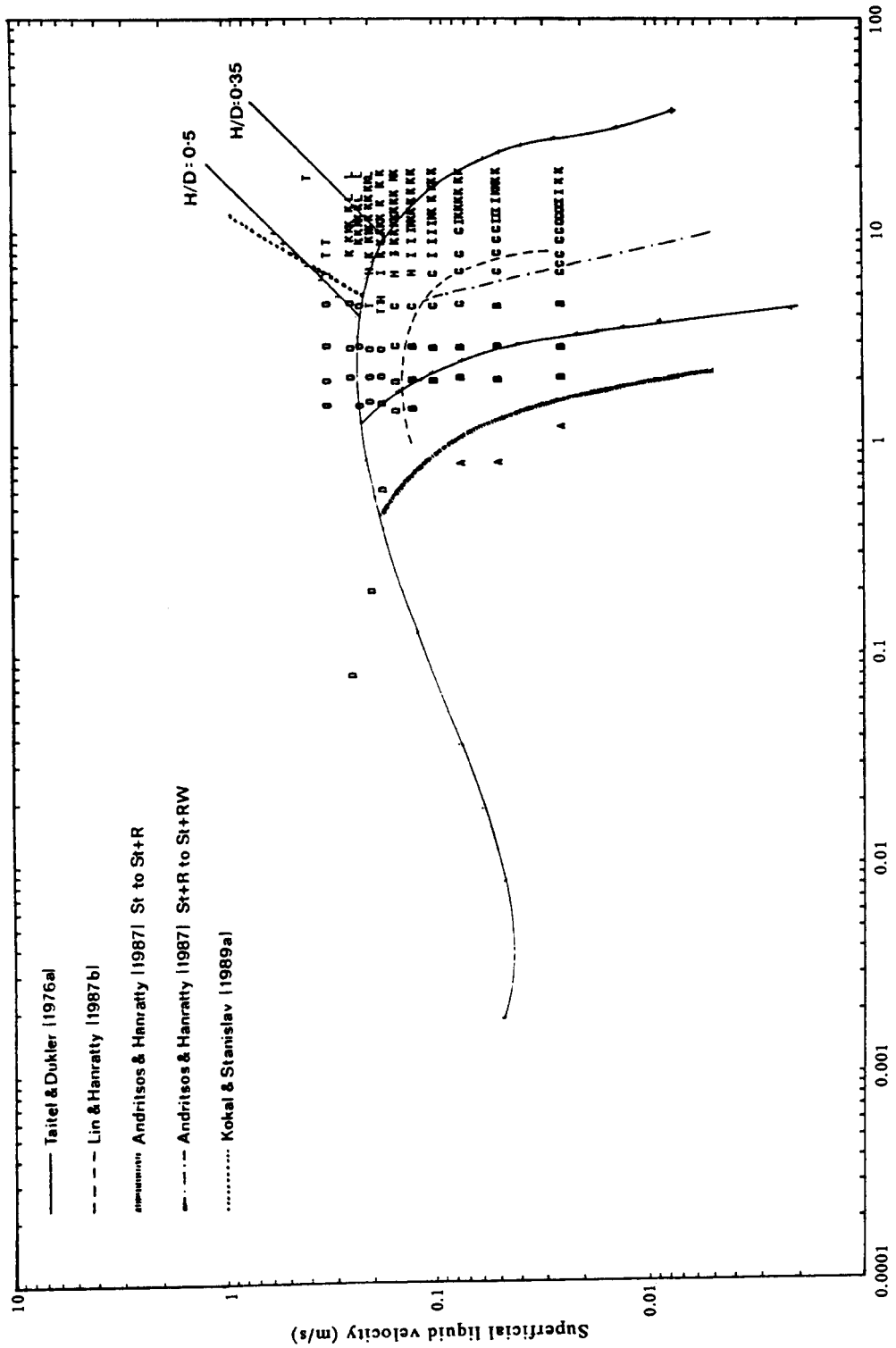

Figure 20. Comparison of theoretical flow pattern transitions with the air–water data of Spedding *et al.* (1989) for a pipe diameter of 0.0935 m. Symbols are detailed in the appendix.

transition tailed off to describe the transition to St + RW flow. In figure 20, for $\bar{V}_{SG} > 3$ m s^{-1}, the transition overpredicted the St + R and St + RW boundary.

It may be possible to build-in the effect of surface tension into the Lin & Hanratty (1986) analysis, resulting in an improved prediction since surface tension stabilizes the liquid and would be expected to move the St to S flow transition to higher values of $\bar{V}_{SL}$. However, Barnea *et al.* (1983) inferred that surface tension effects were negligible for pipe diameters >0.0254 m.

Kokal & Stanislav (1989a) suggested that the relationship between X and h_L/d should be modified by using the Chen (1979) relationship to predict the single-phase pressure loss:

$$\frac{1}{\sqrt{f}} = -4 \log \left\{ \frac{\epsilon}{3.70560} - \frac{5.0452}{\mathrm{Re}_{SL/G}} \log \left[\frac{1}{2.8257} \left(\frac{\epsilon}{d} \right)^{1.1098} + \left(\frac{5.8506}{\mathrm{Re}_{SL/SG} 0.8981} \right) \right] \right\}. \quad [6]$$

The use of the Ellis & Gay (1959) correlation was suggested for the prediction of the interfacial gradient:

$$f_i = 1.3 \, \mathrm{Re}_{SG}^{-0.5}. \quad [7]$$

Kokal & Stanislav (1989a) proposed that the Taitel & Dukler criterion for the transition between St and S flow should be used in conjunction with the values of X and h_L/d generated using [6] and [7]. Their results inferred that there was no significant improvement over the original theory, using $f_i/f_{SG} = 1.0$ and predicting the single-phase pressure loss using the Blasius (1913) relationship.

The transitions from S to A flow are illustrated in figures 19 and 20 for $h_L/d = 0.5$ (Taitel & Dukler 1976a) and $h_L/d = 0.35$ (Barnea *et al.* 1982). The transition for $X = 1.47$ (Barnea & Taitel 1986) was not illustrated since it gave very similar results to the $h_L/d = 0.5$ line. For both of the diameters shown, the $h_L/d = 0.5$ transition line gave a good indication of the change between the S and St + BTS flow patterns. This represented the changes from slugs with discernible fronts, bodies and tails to the frothy BTS pattern where only constriction of the pipe occurred.

Taking a value of $X = 0.7$, which corresponded to $h_L/d = 0.35$, did not improve the prediction of the S to A boundary.

When considering the S to A transition, neither Barnea *et al.* (1982) nor Taitel & Dukler (1976a) observed the gradual change through the BTS flow pattern. Their theories also suggested that the location of the S to A transition was not affected by pipe diameter.

Both Lin & Hanratty (1987b) and Kokal & Stanislav (1989a) have identified the hybrid BTS pattern which caused the transition between S and wavy annular flow to be particularly difficult to determine, since quantitatively distinguishing visually between a highly aerated slug and the A + RW patterns was difficult without recourse to more definitive techniques.

Kokal & Stanislav (1989a) proposed a criterion for the transition between S and A flow, given by

$$\bar{V}_{SG} = 10.36 \, \bar{V}_{SL} + C_1 \quad [8]$$

and

$$C_1 = 2.98 \left[\frac{g \, d(\rho_L - \rho_G)}{\rho_L} \right]^{1/2}. \quad [9]$$

The proposed transition included the effect of diameter. When compared with the data in figures 19 and 20 the criterion gave a good indication of the boundary between the S and BTS regions for the 0.0455 m i.d. pipe. For the 0.0935 m i.d. pipe the accuracy of the prediction diminished with decreasing $\bar{V}_{SL}$. Kokal & Stanislav (1989a) inferred that the transition only located the S to A boundary approximately because of the presence of the BTS.

For the transition between St and St + W patterns, Taitel & Dukler (1976a) modified the condition for wave generation put forward by Jeffreys (1925, 1926):

$$(\bar{V}_G - C_p)^2 \, C_p > \frac{4 \nu_L g (\rho_L - \rho_G)}{s \rho_G}, \quad [10]$$

where C_p is the wave velocity and ν_L is the liquid kinematic viscosity.

The value of the sheltering coefficient, s, was taken as 0.01. Equation [10] was also expressed in dimensionless form as

$$K > \frac{2}{\sqrt{\bar{V}_L}\,\bar{V}_G\sqrt{s}}. \qquad [11]$$

Figures 19 and 20 indicated that this transition criterion was not successful in predicting the St to St + RW flow patterns. Again, the two wave patterns St + R and St + RW were not discussed in the analysis.

Andritsos & Hanratty (1987) examined the interfacial instabilities which existed in stratified flow. They suggested that a sheltering coefficient of 0.06 should be used in [10] to give an approximate representation of the gas velocity to initiate waves on liquids with $\nu < 0.02$ kg m^{-1} s^{-1}. The transitions were plotted in figures 19 and 20. For the 0.0455 m i.d. pipe the boundary was described adequately for $V_{SL} > 0.01$ m s^{-1} but below this the agreement was poor. The amount of St flow data was limited for the 0.0935 m i.d. pipe, but the use of $s = 0.06$ did give a better description of the transition for the particular $\bar{V}_{SL}$ values encountered.

A second wave type was also noted by Andritsos & Hanratty (1987) which was distinguished by a very large increase in interfacial drag. They indicated that the inviscid Kelvin–Helmholtz equation was a good first approximation of the gas velocity $\bar{V}_{KH}$ required to initiate the second wave type; this is given by

$$(\bar{V}_{KH} - \bar{V}_L) > \left(\frac{k_M \rho_L}{\rho_G} + \frac{\rho_L g}{\rho_G k_M}\right)\tanh(k_M h_G), \qquad [12]$$

where

$$k_M = \left(\frac{\rho_L g}{\sigma}\right)^{1/2} \qquad [13]$$

and σ is the surface tension.

An empiricism was introduced to account for the effects or liquid height and liquid viscosity, giving

$$\bar{V}_{SG} = \bar{V}_{KH}\frac{\Delta_w^{0.025}}{\Delta}\left[\tanh\frac{k_M h_L}{10}\right]^{-0.1}\frac{1}{\bar{R}_G}, \qquad [14]$$

where

$$\Delta = \frac{\rho_L}{\rho_G}\frac{\sigma^2}{\mu_L^2 \bar{V}_G^2}. \qquad [15]$$

The term Δ_w was the value of Δ for water.

The transition criteria should have corresponded to the boundary between the St + R and St + RW flows, but this was not the case when compared against the data in figures 19 and 20.

WEISMAN *et al.* (1979) CORRELATIONS

Weisman *et al.* (1979) proposed a series of flow pattern transitions which were tested with data which covered a wide range of fluid properties, and pipe diameters of 0.012, 0.025 and 0.051 m. Correlations were given for the following transition boundaries:

separated to intermittent transition,

$$\frac{\bar{V}_{SG}}{\sqrt{gd}} = 0.25\left(\frac{\bar{V}_{SG}}{\bar{V}_{SL}}\right)^{1.1}; \qquad [16]$$

transition to A flow,

$$1.9\left(\frac{\bar{V}_{SG}}{\bar{V}_{SL}}\right)^{1.8} = \left\{\frac{\bar{V}_{SG} G^{0.5}}{[g(\rho_L - \rho_G)\sigma]^{0.25}}\right\}^{0.2}\left(\frac{\bar{V}_{SG}^2}{gd}\right)^{0.18}; \qquad [17]$$

transition to dispersed bubble,

$$\left[\frac{\left(\frac{dP}{dl}\right)_{SL}}{(\rho_L-\rho_G)g}\right]^{1/2}\left[\frac{\sigma}{(\rho_L-\rho_G)gd^2}\right]^{-1/4}=1.7; \qquad [18]$$

stratified smooth to stratified wavy transition

$$\left[\frac{\sigma}{gd^2(\rho_L-\rho_G)}\right]^{0.2}\left(\frac{d\bar{V}_{SG}\rho_G}{\mu_G}\right)^{0.45}=8\left(\frac{\bar{V}_{SG}}{\bar{V}_{SL}}\right)^{0.16}. \qquad [19]$$

All of these transition criteria, with the exception of the transition to dispersed bubble, were compared with the data collected for the 0.0455 and 0.0935 m i.d. pipes in figures 21 and 22, respectively. Generally, the agreement between the experimental data and the proposed transitions was poor, with the expection of the St to St + W criterion, which gave a good prediction of the St to St + RW transition.

KADAMBI (1982) MODEL

Kadambi (1982) considered the A to St transition by solving the momentum balances for both flows for similar gas and liquid input conditions. It was concluded that the pressure changes which occur during the transition from A to St flow, P_R, were given by

$$\frac{\Delta P_R}{\rho_L\bar{V}_{L1}^2}=(\bar{R}_{G2}-\bar{R}_{G1})\left[\frac{\bar{R}_{L1}}{\bar{R}_{L2}}-\frac{\rho_G}{\rho_L}\cdot\left(\frac{\bar{V}_{G1}}{\bar{V}_{L1}}\right)^2\cdot\frac{\bar{R}_{G1}}{\bar{R}_{G2}}\right]+\frac{1}{\pi Fr_K^2}$$

$$\cdot\left[\sin\eta\frac{(1-\sin^2\eta)}{3}-\eta\cos\eta-\frac{\pi h\bar{R}_{L1}}{2'r}\right]+\frac{\bar{R}_{L1}}{We_K\bar{R}_{G1}^{0.5}}. \qquad [20]$$

The subscript 1 denoted annular conditions and the subscript 2 denoted stratified flow. The quantities We_K and Fr_K were the Weber and Froude numbers, defined as follows:

$$Fr_K=\frac{\bar{V}_{L1}}{(g'r)^{0.5}} \qquad [21]$$

and

$$We_K=\frac{\bar{V}_{L1}^2\rho_L'r}{\sigma}. \qquad [22]$$

The quantities h, and η were given by

$$h='r(1-\sqrt{\bar{R}_{G1}}) \qquad [23]$$

and

$$\bar{R}_{G2}=1-\left(\frac{\eta-\frac{\sin 2\eta}{2}}{\pi}\right), \qquad [24]$$

where $'r$ was the pipe radius.

It was stated that for stable A flow to exist the A gas holdup should be greater than that for St flow for similar input conditions. So the kinetic energy of the gas was less in the A than in the St condition. The final transition criteria were:

$$\frac{\left(\frac{\rho_G}{\rho_L}\right)\left(\frac{\bar{V}_{G1}}{\bar{V}_{L1}}\right)^2(\bar{R}_{G1}^2-\bar{R}_{G2}^2)}{2\bar{R}_{G2}^2}-\frac{\Delta P_R}{\rho_L\bar{V}_{L1}^2}>0. \qquad [25]$$

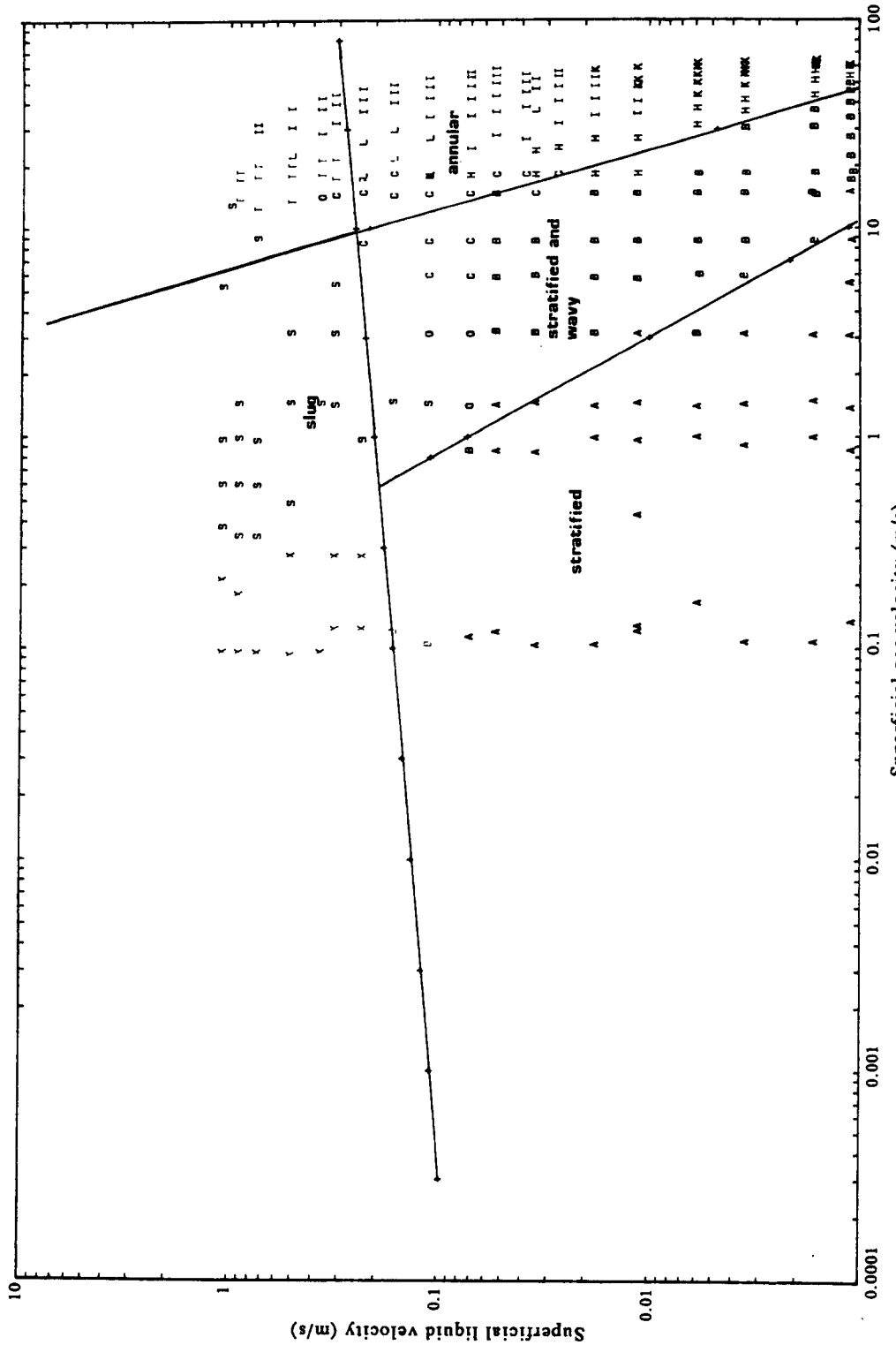

Figure 21. Flow pattern transitions due to Weisman *et al.* (1979) compared with the air–water data of Spedding *et al.* (1989) for a pipe diameter of 0.0455 m. Symbols are detailed in the appendix.

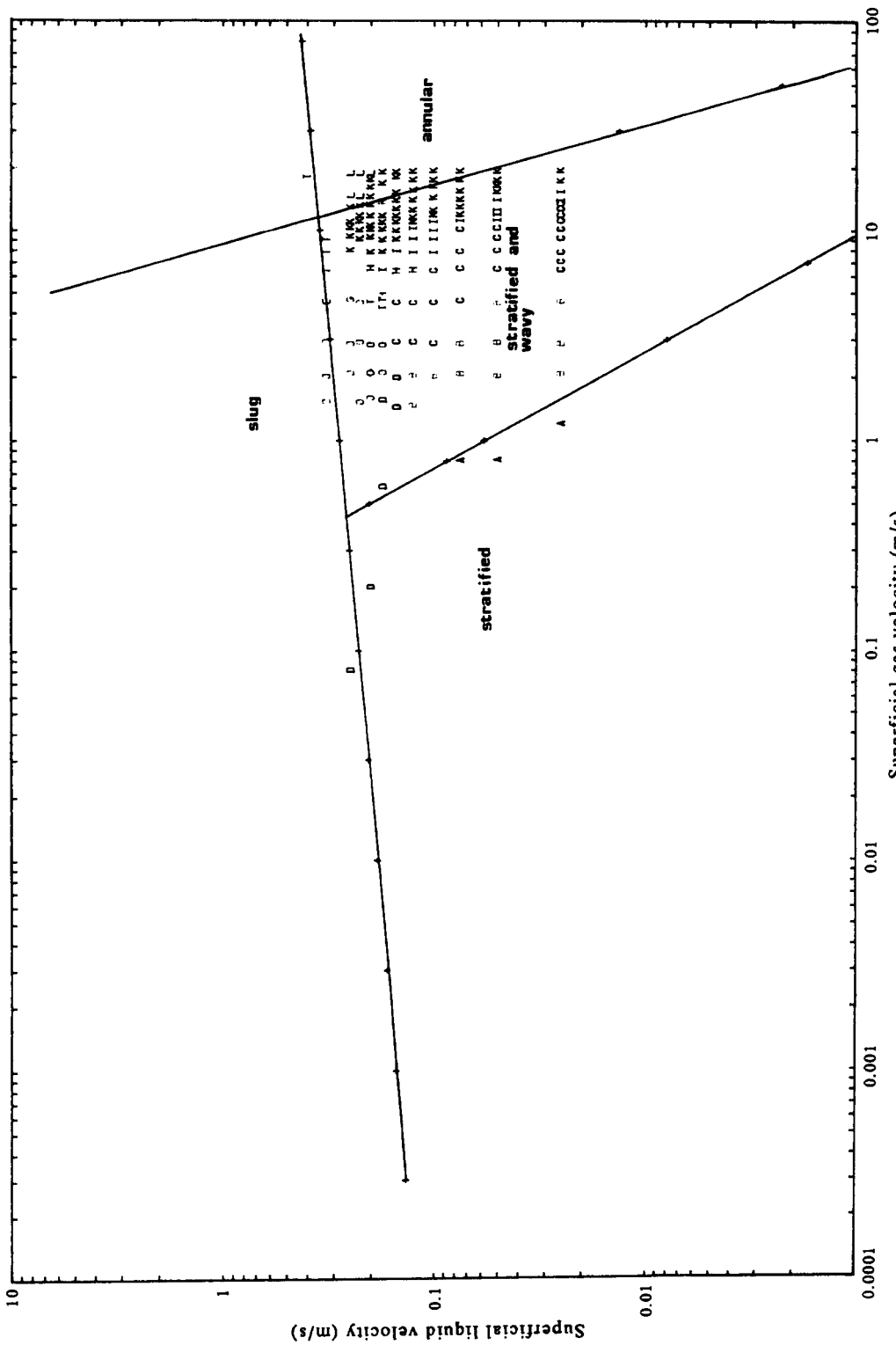

Figure 22. Flow pattern transitions due to Weisman *et al.* (1979) compared with the air–water data of Spedding *et al.* (1989) for a pipe diameter of 0.0935 m. Symbols are detailed in the appendix.

The transition was established by calculating the A and St holdups, ΔP_R and, finally, the transition criteria from [25].

For the prediction of the holdup in St flow the method suggested by Kadambi (1981) was recommended. This model utilized the Pai (1953) velocity profile:

$$\frac{V_p}{V_{MAX}} = 1 + a_1\left(\frac{r}{'r}\right)^2 + a_2\left(\frac{r}{'r}\right)^{2n}, \quad [26]$$

where

$$a_1 = \frac{b-n}{n-1} \quad [27]$$

and

$$a_2 = \frac{1-b}{n-1}. \quad [28]$$

The Pai (1953) velocity profile and the Brodkey (1963) correlations for b and n were found to predict the point velocity, V_p, accurately up to an $r/'r$ value of 0.9 but not beyond; hence at points close to the pipe wall the predictions of the point velocity were poor. This gave rise to errors in the prediction of $\bar{R}_{L2}$ when the liquid stratified layer was thin, because the model relied on the matching of the gas and liquid velocity at the interface. Since the velocity profile used was not accurate in this region there may be considerable errors when using the procedure. This became apparent when the correlation was compared with experimental data, as shown in Table 1: where the average error in the prediction of either gas or the liquid holdup in St flow was small, the spread in errors was unacceptably large.

The A flow model due to Kadambi (1985) applied a similar procedure based on the Pai (1953) velocity profiles and hence must suffer from similar errors.

Kadambi (1982) further suggested that for a given pipe diameter there was a specific value of liquid superficial Reynolds number, $\bar{R}e_{SL}$, below which a systematic increase in the gas rate could not result in the production of the A flow pattern. It was also apparent that for larger pipe diameters the characteristic $\bar{R}e_{SL}$ should have a larger value. This trend had also been observed by Taitel & Dukler (1976a) and Weisman *et al.* (1979).

The characteristic $\bar{V}_{SL}$ and $\bar{V}_{SG}$ values which described the boundary of the stable region for A flow (for air–water data with pipe diameters of 0.051 and 0.102 m) were compared with the data obtained by Spedding *et al.* (1989), for pipes of 0.0455 and 0.0935 m i.d., in figures 23 and 24. However, in figures 23 and 24 the stable regions of A flow were much larger than that suggested by the data. Such an effect was noted by Kadambi (1982) and it was proposed that the accuracy could be improved by incorporating into the model dissipative and frictional effects which occurred during the transition.

The minimum $\bar{V}_{SL}$ which must be attained for A flow to occur was also plotted in figures 23 and 24. These were deduced from the minimum values of $\bar{R}e_{SL}$ presented by Kadambi (1982) for both

Table 1. Errors in the prediction of holdup using the stratified flow model of Kadambi (1981) compared against the air water data of Spedding *et al.* (1989)

	$\bar{R}_L$		$\bar{R}_G$	
Flow type	Spread (%)	Ave. error (%)	Spread (%)	Ave. error (%)
St	+250, −90	5	+30, −50	−5
St + R	+100, −90	−65	+25, −25	2
St + RW	120, −80	50	+5, −20	−10
St + IW	+30, −30	30	−50, −50	−50
F + D	+120, −90	−60	+5, −10	+3
A + D	+110, −80	50	+2, −25	−5
D	−80, −90	−85	+1, 0	0.5
A + RW	+130, −90	+70	+2, −20	−10
BTS + St	+70, +20	+50	−10, −25	−15
BTS + A	+110, +85	+90	−15, −30	−20
S	+130, +15	+70	−30, −70	−55
B	+40, +3	+15	−25, −70	−40

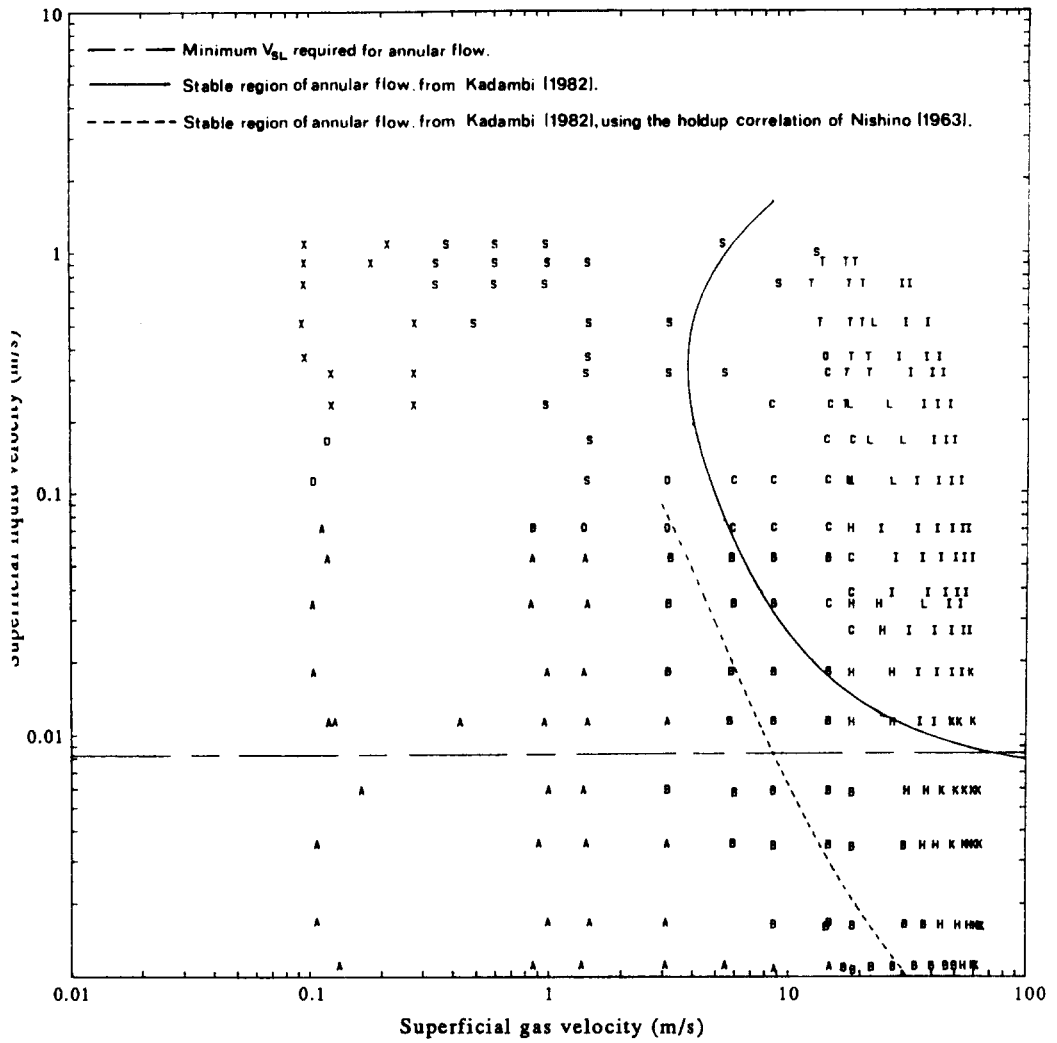

Figure 23. Stable region of A flow, due to Kadambi (1982), compared with the air–water data of Spedding *et al.* (1979) for a pipe diameter of 0.0455 m. Symbols are detailed in the appendix.

the 0.051 and 0.102 m i.d. pipes. The value of the minimum $\bar{V}_{SL}$ was predicted accurately for the 0.0455 m i.d. pipe, even allowing for the small difference in diameter, however a lower value of $\bar{V}_{SL}$ was predicted for the 0.102 m i.d. pipe, as shown in figure 24.

Such a result was not expected, since for larger pipe diameters the transition from S to A flow takes place at higher $\bar{V}_{SL}$—suggesting that the minimum $\bar{V}_{SL}$ above which A flow should occur should also increase. This is in line with the experimental findings of Lin & Hanratty (1987b), who determined that for similar values of $\bar{V}_{SL}$ the h/d ratio of interfacial waves was greater for smaller diameter pipes. By following such reasoning, it would be expected that atomization would occur at lower $\bar{V}_{SL}$ and hence, the smaller the diameter, the lower the value of $\bar{V}_{SL}$ at which the entrainment and redeposition method of sustaining A flow would occur.

In figures 23 and 24 the transitions were determined theoretically using [20]–[25]. The gas holdup in St flow was determined using the recommended method of Kadambi (1981). The A gas holdup was predicted using the correlation due to Nishino & Yamasaki (1963), which was found by Spedding & Spence (1988) to give a good prediction of both the gas and liquid holdup for A + D and A + RW flows. From figures 23 and 24 it was evident that the position of the transition line changed depending on the holdup correlation method used to predict the A gas and liquid holdup. This may have explained the poor prediction of the transition for oil–gas flows which was mentioned by Kadambi (1981), since the holdup prediction methods may not be accurate for such a fluid system.

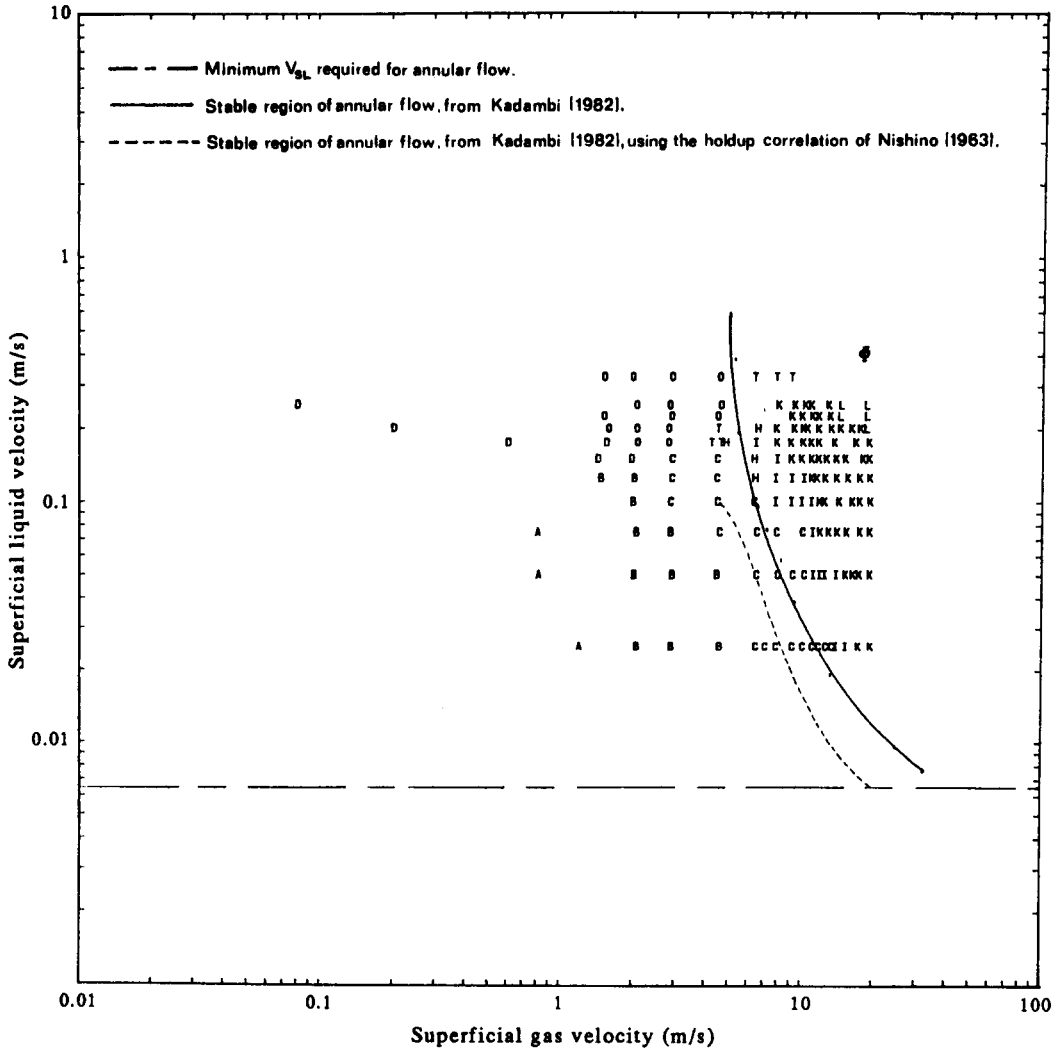

Figure 24. Stable region of A flow, due to Kadambi (1982), compared with the air–water data of Spedding *et al.* (1979) for a pipe diameter of 0.0935 m. Symbols are detailed in the appendix.

The theory indicated that the transition to A flow occurred due to an energy exchange at the gas–liquid interface, without specifying the mechanism for transfer. Such a postulation suggested that entrainment and redeposition had no effect on the transition. This did not agree with observations of both Lin & Hanratty (1987b) and Anderson & Russell (1970a,b), where the transition to A flow for low $\bar{V}_{SL}$ took place due to entrainment and redeposition, and for higher $\bar{V}_{SL}$ due to disturbance waves/BTS flow patterns. These different mechanisms were not accounted for by the model and, again, this indicated errors in the prediction of the transition when using this procedure.

CONCLUSION

Experimental data are provided for two-phase air–water co-current flow in a 0.0935 m i.d. pipe. Flow regimes were identified by a combination of visual/video observations, pressure loss and holdup data examinations and pressure loss fluctuating characteristics.

Existing regime maps and theories for the prediction of phase boundary transitions did not satisfactorily predict observed flow pattern regimes, particularly when the geometrical parameters and physical properties of the phases were varied. Therefore, another different approach has been developed for the problem of flow pattern prediction.

REFERENCES

ALVES, G. E. 1954 Cocurrent liquid gas flow in a pipeline contractor. *Chem. Engng Prog.* **50,** 449–456.

ANDERSON, R. J. & RUSSELL, T. W. F. 1970a Film formation in two phase annular flow. *AIChE Jl* **16,** 626–633.

ANDERSON, R. J. & RUSSELL, T. W. F. 1970b Circumferential variation of interchange in horizontal annular two phase flow. *Ind. Engng Chem. Fundam.* **9,** 340–343.

ANDRITSOS, N. & HANRATTY, T. J. 1987 Interfacial instabilities for horizontal gas–liquid flow in pipelines. *Int. J. Multiphase Flow* **13,** 583–603.

ANNUNZIATO, M. & GIRARDI, G. 1985 Characterisation of horizontal two phase flow in large diameter tubes. Paper presented at the *European Two Phase Flow Gp Mtg*, Southampton, U.K.

ANNUNZIATO, M. & GIRARDI, G. 1986 Two phase flow pattern recognition in straight tubes. Paper presented at the *European Two Phase Flow Gp Mtg*, Munich, Germany.

ARMAND, A. A. 1946 The resistance during the movement of a two phase system in horizontal pipes. *Izv. Vses. Teplotekh. Inst.* **1,** 16–23.

AZZOPARDI, B. J. & RUSSELL, C. M. B. 1984 Two phase flow patterns in horizontal tubes at high qualities. Paper presented at the *2nd Natn. Congr. on Heat Transfer*, Bologna, Italy.

BAKER, O. 1954 Simultaneous flow of oil and gas. *Oil Gas J.* **26 July,** 185–195.

BARNEA, D. 1987 A unified model for predicting flow pattern transitions for the whole range of pipe inclinations. *Int. J. Multiphase Flow* **13,** 1–12.

BARNEA, D. & BRAUNER, N. 1985 Holdup of the slug in two phase intermittent flow. *Int. J. Multiphase Flow* **11,** 43–49.

BARNEA, D. & TAITEL, Y. 1986 Flow pattern transitions in two phase gas–liquid flows. In *Encyclopedia of Fluid Mechanics*, Vol. III (Edited by CHEREMISINOFF, N. P.), pp. 403–474. Gulf, Houston, TX.

BARNEA, D., SHOHAM, O. & TAITEL, Y. 1980a Flow pattern characterisation in two phase flow by electrical conductance probes. *Int. J. Multiphase Flow* **6,** 387–397.

BARNEA, D., SHOHAM, O., TAITEL, Y. & DUKLER, A. E. 1980b Flow pattern transitions for gas–liquid flow in horizontal and inclined pipes; comparison of experimental data with theory. *Int. J. Multiphase Flow* **6,** 217–225.

BARNEA, D., SHOHAM, O. & TAITEL, Y. 1982 Flow pattern transitions for downward inclined two phase flow: horizontal to vertical. *Chem. Engng Sci.* **37,** 735–740.

BARNEA, D., LUNISKI, Y. & TAITEL, Y. 1983 Flow patterns in horizontal and vertical two phase flow in smaller diameter pipes. *Can. J. Chem. Engng* **61,** 617–620.

BISHOP, A. A. & DESHPANDE, S. D. 1986 Interfacial level gradient effects in horizontal Newtonian liquid–gas stratified flow—I. *Int. J. Multiphase Flow* **12,** 957–975.

BLASIUS, H. 1913 Das ahnlichkeitsgestz, bei Reibungsvorgangen in flussigbeiten. *Forschft. Ver. Deut. Int.* **131,** 123–139.

BRILL, J. P., SCHMIDT, Z., COBERLY, W. A., HERRING, J. D. & MOORE, D. W. 1981 Analysis of two phase tests in large diameter flow lines in the Prudoe Bay field. *Soc. Pet. Engrs* **June,** 363–378.

BRODKEY, R. S. 1963 Limitations of a generalised velocity distribution. *AIChE Jl* **9,** 448–451.

BUTTERWORTH, D. 1971 Air–water, annular flow in a horizontal tube. Report AERE-R6687.

BUTTERWORTH, D. & PULLING, D. J. 1972 A visual study of the mechanisms in horizontal, annular air–water flow. Report AERE-M2556.

CHEN, N. H. 1979 An explicit equation for friction factor in pipes. *Ind. Engng Chem Fundam.* **18,** 269–297.

CHURCHILL, S. W. 1977 Friction equation spans all flow regimes. *Chem. Engng (N.Y.)* **84,** (24) 91–92.

CROWLEY, C. J., SAM, R. G., WALLIS, G. B. & MEHTA, D. C. 1985 Slug flow in a large diameter pipe: the effect of fluid properties. Paper presented at the *AIChE A. Mtg*, San Francisco, CA.

DALLMAN, J. C., LAURINAT, J. E. & HANRATTY, T. J. 1984a Entrainment for horizontal gas liquid flow. *Int. J. Multiphase Flow* **10,** 677–690.

DALLMAN, J. C., LAURINAT, J. E. & HANRATTY, T. J. 1984b Pressure drop and film height measurements for annular gas–liquid flow. *Int. J. Multiphase Flow* **10,** 341–356.

DUKLER, A. E. & HUBBARD, M. G. 1975 A model for gas–liquid slug flow in horizontal and near horizontal tubes. *Ind. Engng Chem. Fundam.* **14,** 337–347.

ELLIS, S. R. M. & GAY, B. 1959 The parallel flow of two fluid streams: interfacial shear and fluid fluid interaction. *Trans. Inst. Chem. Engrs* **37,** 206–213.

FAIRHURST, C. P. 1988 Slug flow behaviour classified in large diameter pipeline study. *Oil Gas J.* **3 Oct.,** 49–57.

GAY, R. R., BROCKETT, G. R. & JOHNSTON, R. I. 1978 Two phase flow measurement techniques in nuclear safety research. In *Two Phase Flow and Reactor Safety*, Vol. III (Edited by VEZIROGLU, T. N. & KAKAC, S.) Hemisphere, Washington, DC.

GAZLEY, C. 1948 Interfacial shear and stability in two phase flow. Ph.D. Thesis, Univ. of Delaware, Newark, DE.

GERAETS, J. J. M. & BORST, J. C. 1988 A capacitance sensor for two phase void fraction measurements and flow pattern identification. *Int. J. Multiphase Flow* **14,** 305–320.

HEWITT, G. F. 1982 Liquid–gas system. In *The Handbook of Multiphase Systems* (Edited by HETSRONI, G.). McGraw-Hill, New York.

HOOGENDOORN, C. J. 1959 Gas–liquid flow in horizontal pipes. *Chem. Engng Sci.* **9,** 205–217.

ISHII, M. 1982 Wave phenomena and two phase flow instabilities. In *The Handbook of Multiphase Systems* (Edited by HETSRONI, G.). McGraw-Hill, New York.

JEFFREYS, H. 1925 On the formation of waves by wind. *Proc. R. Soc.* **A107,** 189–201.

JEFFREYS, H. 1926 On the formation of waves by wind. *Proc. R. Soc.* **A110,** 241–268.

JENKINS, R. 1947 Two phase two component flow of air and water. M.Sc. Thesis, Univ. of Delaware, Newark, DE.

JEPSON, W. P. 1987 Transition to slug flow in a horizontal conduit. Report AERE-R12813.

JONES, O. C. & ZUBER, N. 1975 The interrelation between void fraction fluctuations and flow pattern in two phase flow. *Int. J. Multiphase Flow* **2,** 273–306.

KADAMBI, V. 1981 Void fraction and pressure drop in two phase stratified flow. *Can. J. Chem. Engng* **59,** 585–589.

KADAMBI, V. 1982 Stability of annular flow in horizontal flow. *Int. J. Multiphase Flow* **8,** 317–328.

KADAMBI, V. 1985 Prediction of pressure drop and void fraction in annular two phase flow. *Can. J. Chem. Engng* **63,** 728–734.

KOKAL, S. L. & STANISLAV, J. F. 1989a An experimental study of two phase flow in slightly inclined pipes: I—flow patterns. *Chem. Engng Sci.* **44,** 665–679.

KOKAL, S. L. & STANISLAV, J. F. 1989b An experimental study of two flow in slightly inclined pipes: II—liquid holdup and pressure drop. *Chem. Engng Sci.* **44,** 681–693.

KORDBYAN, E. S. 1977a Some characteristics of high waves in closed channels approaching the Kelvin–Helmholtz instability. *ASME Jl Bas. Engng, Ser. D* **99,** 339–346.

KORDBYAN, E. S. 1977b Brief Communication: the transition to slug flow in the presence of large waves. *Int. J. Multiphase Flow* **3,** 603–607.

KORDBYAN, E. S. 1985 Some details of developing slugs in horizontal two phase flow. *AIChE Jl* **31,** 802–806.

KORDBYAN, E. S. & RANOV, T. 1970 Mechanisms of slug formation in horizontal two phase flow. *ASME Jl Bas. Engng, Ser. D* **92,** 857–864.

KOSTERIN, S. I. 1949 An investigation of the influence of the diameter and inclination of a tube on the hydraulic resistance and flow structure of gas liquid mixtures. *Izv. Akad. Nauk SSSR, Otdel Tekh. Nauk* **12,** 1824–1830.

LIN, P. Y. & HANRATTY, T. J. 1986 Prediction of the initiation of slugs with linear stability theory. *Int. J. Multiphase Flow* **12,** 79–88.

LIN, P. Y. & HANRATTY, T. J. 1987a Detection of slugs from pressure measurements. *Int. J. Multiphase Flow* **13,** 13–21.

LIN, P. Y. & HANRATTY, T. J. 1987b The effect of pipe diameter on flow patterns for air water flow in horizontal pipes. *Int. J. Multiphase Flow* **13,** 549–563.

MANDHANE, J. M., GREGORY, G. A. & AZIZ, K. 1974 Flow pattern map for gas–liquid flow in horizontal pipes. *Int. J. Multiphase Flow* **1,** 537–553.

NISHINO, H. & YAMASAKI, Y. 1963 *J. Soc. Atom. Energy Japan* **5,** 39–52.

NGUYEN, V. T. 1975 Two phase flow. Ph.D. Thesis, Univ. of Auckland, New Zealand.

PAI, S. I. 1953 On turbulent flow in a circular pipe. *J. Franklin Inst.* **256,** 337–352.

RUDER, Z., HANRATTY, P. J. & HANRATTY, T. J. 1989 Necessary conditions for the existence of stable slugs. *Int. J. Multiphase Flow* **15,** 209–226.

RUSTON, J. H., COSTICH, E. W. & EVERETT, H. J. 1950 Power characteristics of mixing impellers. *Chem. Engng Prog.* **46,** 395–398, 467–471.

SCHICHT, H. H. 1969 Flow patterns for an adiabatic two-phase flow of water and air within a horizontal tube. *Verfarenstechnik* **3,** 153–169.

SCOTT, D. S. 1963 Properties of cocurrent gas–liquid flow. *Adv. Chem. Engng* **4,** 199–277.

SEKOGUCHI, K., OUSAKA, A., FUKANO, T. & MORIMOTO, T. 1982 Air–water annular two phase flow in a horizontal tube. *Bull. JSME* **25,** 1559–1565.

SPEDDING, P. L. & NGUYEN, V. T. 1980 Regime maps for air-water two phase flow. *Chem. Engng Sci.* **35,** 779–793.

SPEDDING, P. L. & SPENCE, D. R. 1988 Prediction of holdup in two phase flow. *Int. J. Fluid Mech.* **1,** 67–82.

SPEDDING, P. L. & SPENCE, D. R. 1991 A novel approach to flow regime prediction in gas–liquid sysetms. *Dev. Chem. Engng SST* **14,** 94–116.

SPEDDING, P. L., HAND, N. P. & SPENCE, D. R. 1989 Data on horizontal, co-current, two phase gas–liquid flows. Report CE/1/89, Queen's Univ., Belfast, N. Ireland.

TAITEL, Y. 1977 Brief Communication: flow pattern transitions in rough pipes. *Int. J. Multiphase Flow* **3,** 597–601.

TAITEL, Y. & DUKLER, A. E. 1976a A model for predicting flow regime transitions in horizontal and near horizontal gas–liquid flow. *AIChE Jl* **22,** 47–55.

TAITEL, Y. & DUKLER, A. E. 1976b A theoretical approach to the Lockhart, Martinelli correlation for stratified flow. *Int. J. Multiphase Flow* **2,** 591–595.

TRONIEWSKI, L. & ULBRICH, R. 1984 An analysis of flow regime maps of two phase gas–liquid flows in pipelines. *Chem. Engng Sci.* **39,** 1225–1231.

VINCE, M. A. & LAHEY, R. T. 1982 On the development of an objective flow regime indicator. *Int. J. Multiphase Flow* **8,** 93–124.

VOHR, J. 1960 Flow patterns of two phase flow—a literature survey. Report TID-11514, Columbia Univ., New York (1960).

WALLIS, G. B. & DOBSON, J. E. 1973 The onset of slugging in horizontal stratified air–water flow. *Int. J. Multiphase Flow* **1,** 173–179.

WEISMAN, J., DUNCAN, D., GIBSON, J. & CRAWFORD, T. 1979 Effects of fluid properties and pipe diameter on two phase flow patterns in horizontal lines. *Int. J. Multiphase Flow* **5,** 437–462.

APPENDIX

0.0935m i.d. Pipe, Air–Water Data after Spedding et al. (1989)

Stratified	A
Stratified + ripple	B
Stratified + roll wave	C
Stratified + inertial wave	D
Stratified + large roll wave + droplet	H
Stratified + roll wave + droplet	I
Film + droplet	K
Annular + roll wave	L
Slug	O
Stratified + blow through slug	T
Annular + blow through slug	

0.0455m i.d. Pipe, Air–Water Data after Spedding et al. (1989)

Stratified	A
Stratified + ripple	B
Stratified + roll wave	C
Stratified + inertial wave	D
Film + droplet	H
Annular + droplet	I
Droplet	K
Annular + roll wave	L
Stratified + blow through slug	O
Annular + blow through slug	T
Slug	S
Bubble	X